Wave resource assessment for Scottish waters using a large scale North Atlantic spectral wave model

Citation for published version:
Venugopal, V & Nemalidinne, R 2015, 'Wave resource assessment for Scottish waters using a large scale North Atlantic spectral wave model', *Renewable Energy*, vol. 76, pp. 503-525.
https://doi.org/10.1016/j.renene.2014.11.056

Digital Object Identifier (DOI):
10.1016/j.renene.2014.11.056

Published In:
Renewable Energy

Wave Resource Assessment for Scottish Waters Using a Large Scale North Atlantic Spectral Wave Model

Vengatesan Venugopal* and **Reddy Nemalidinne**

Institute for Energy Systems, School of Engineering
The University of Edinburgh, Edinburgh, EH9 3JL
United Kingdom

Abstract

This paper reports the methodology established in the application of a numerical wave model for hindcasting of wave conditions around the United Kingdom, in particular for Scottish waters, for the purpose of wave energy resource assessment at potential device development sites. The phase averaged MIKE21 Spectral wave model has been adopted for this study and applied to the North Atlantic region bounded by latitudes 10^o N - 70^o N and longitudes 10^o E-75^o W. Spatial and temporal wind speeds extracted from the European Centre for Medium Range Weather Forecast (ECMWF) have been utilised to drive the wave model. A rigorous calibration and validation of the model has been carried out by comparing model results with buoy measurements for different time periods and locations around Scotland. Significant wave height, peak wave period and peak wave direction obtained from the model correlated very well with measurements. Spatially varying statistical mean and maximum values of the significant wave height and wave power obtained based on a one-year wave hindcasting are in good agreement with the UK Marine Atlas values. The wave model can be used with high level of confidence for wave hindcasting and even forecasting of various wave parameters and wave power at any desired point locations or for regions. The wave model could also be employed for generating boundary conditions to small scale regional wave and tidal flow models.

Keywords: Wave modelling, Spectral wave model, Orkney and Pentland waters, hindcasting, wave power, wave parameters.

* Corresponding Author, V.Venugopal@ed.ac.uk

1. Introduction

Electricity generation from ocean waves and tidal current is an active research worldwide and a number of successful technologies are now being investigated in many parts of the globe. Several of these wave/tide power converters, are either being installed and tested currently or already connected to grids (reNews [1]). According to reNews, the total wave and tidal technologies installed in Scotland alone until now sums to 6.365 MW, and the rest of the countries in the world contributed to only 6.56 MW. The Pentland Firth (see Figure 1), which is the region between the north-east tip of Scotland and the south of Orkney Islands, is considered to be one of the best sites in the world for generating electricity from tidal stream. Figure 1 also indicates the strategic potential sites, licensed by the Crown Estate [2], where wave and tidal energy devices will be deployed by various developers.

In Scotland, the Aquamarine Power [3] installed its Oyster 800 wave power machine at the European Marine Energy Centre (EMEC) facility in Orkney at a water depth of 13 m and commenced operational testing in June 2012. The company claims it produced the first electrical power to the grid in the same month. The company is likewise planning to deploy its next-generation machine Oyster 801 side by side, thus creating a wave farm. In addition, the Aquamarine Power now has been consented from the Scottish Government to develop a 40MW wave farm off the north-west coast of Lewis, Scotland, which will include the deployment of 40 to 50 Oyster devices along the coast of Lewis.

Pelamis Wave Power [4], another wave device developer, has also deployed and tested its Pelamis P2 machine at the EMEC facility in Orkney, the Billia Croo test site, for Scottish Power Renewables. The Pelamis P2 was installed at EMEC for the first time in May 2012 at a water depth of approximately 50 m. Pelamis wave power plans to install 66 Pelamis machines for a 50 MW production off the Marwick Head in Orkney, for which the company claims to have an agreement for lease awarded by the Crown Estate. In addition to the above two, few other wave and tidal power companies, eg., Alstom [5], Andritz Hydro Hammerfest [6], AW Energy technologies [7] , Voith Hydro [8] and Wello Oy [9], have also tested their technologies at EMEC sites. Further details may be found in [10] for tidal power and [11] for wave power technologies.

As demonstrated above, Scotland, in particular Orkney, Pentland Firth and Outer Hebrides, indeed, have become potential regions where both wave and tidal energy technologies can be successfully installed and operated. Scotland is geographically well placed on the globe where large energetic waves from the North Atlantic Ocean provide high level of sustainable wave power resources; however, harvesting these energy sources increase the number of challenges associated with it. An accurate estimation of wave conditions is essential not only for the evaluation of wave power, but also to estimate normal operational and extreme wave scenarios for assessing the survivability and economic viability of the technology and predicting any associated risks.

The UK target is to source 15% of its energy from renewables by 2020, with a commitment to target an 80% reduction in CO_2 emissions by 2050. The Scottish Government has committed to the development of a successful marine renewable energy industry in Scotland and targeting to achieve 20% of European Union's energy consumption from renewable sources by the year 2020 [12]. Scotland’s target is to produce up to a 25% of Europe's tidal power and 10% of its wave power from the seas around it.

To speed up these targets, several funding schemes have been developed and the UK’s Engineering and Physical Sciences Research Council (EPSRC), under its SUPERGEN Marine Challenge - Accelerating the Deployment of Marine Energy (Wave and Tidal) scheme, has funded several projects one of which is the ‘TeraWatt: Large Scale Interactive coupled 3D Modelling for Wave and Tidal Energy Resource and Environmental Impact’ consortium. The work reported in this paper is part of the research carried out for the TeraWatt project which would concentrate on the questions: (i) what is the best way to assess the wave and tidal resource and the effects of energy extraction, (ii) what are the physical consequences of wave and tidal energy extraction and (iii) what are the ecological consequences of wave and tidal energy extraction. In order to address the above questions, an accurate wave and or tidal resource mapping must be produced for the regions where technology deployment activities are planned.

Although, there have been several wave modelling studies carried out in the past for North Atlantic and the UK seas, the purpose of them were manifold. For example, Swail et al., [13] and Swail et al., [14] investigated the longer term variation in ocean wave parameters for North Atlantic using a discrete spectral type wave model called OWI 3-G driven by the NCEP/NCAR global reanalysis wind data. Dodet et al., [15] studied the variability in the North-East Atlantic Ocean using a 57-year hindcast (1953–2009), obtained with the wave model WAVEWATCH III (Tolman, [16]), which was forced with 6-hours wind fields from the NCEP/NCAR Reanalysis project. The spatial resolution of the wind input used for this work was 1.875^{o} (longitude) by 1.905^{o} (latitude) on a Gaussian grid. Their aim was to investigate changes in significant wave height, mean wave direction and peak wave period. Galanis et al [17] explored the characteristics of significant wave height by statistical approach for North Atlantic Ocean using satellite records and simulated records using the WAM wave model (WAMDI Group [18]). They have produced

North Atlantic wide Weibull distribution's 'shape parameters' and 'scale parameters' which would fit the significant wave height hindcast by WAM and also from the satellite records.

Numerical models potentially play several important roles in the assessment of marine energy resources and they also serve to identify commercially exploitable sites. An UK wide wave power resource Atlas has already been produced by ABPmer [19], however the limitations with this Atlas, is that, this was produced based on the wave information made available from the UK Met Office's UK Waters Wave model with a spatial resolution of 12 km and Global Wave Model with a spatial resolution of 60 km. While sufficiently useful information can be obtainable from this Atlas, for specific sites or regions such as Orkney and Pentland Firth where the sea bathymetry is highly variable within a short horizontal space, and also considering future large array scale developments which might require wave information on a spatial scale less than 12 km, it becomes obvious that development of a finer scale wave model capable of accurately providing wave conditions in shallow, intermediate and deep water depths is highly essential, which is what attempted in this work. While a large number of public domain numerical wave models are available, based on the industry partners discretion within the TeraWatt consortium, it has been recommended to use the commercially available MIKE 21 suite [20] for this research, as the results produced could be adaptable by the industry partners for their use as MIKE 21 suite appears to be a common popular and highly preferable tool among them. For the present work the authors propose to use the commercial software MIKE 21 spectral wave model [20] with wind input at 0.125 by 0.125 deg resolutions, for hindcasting wave conditions and wave power for North Atlantic ocean, but focussing mainly on the potential wave energy development locations around Scotland.

An overview of the wave model, bathymetry and mesh construction, methodology adopted in selecting parameters which describe model physics, boundary conditions, calibration and validation of the model to various locations and time periods, analysis of results and the evaluation of performance indices etc, have been detailed in the sections below. It is anticipated that this model would be very useful for hindcasting and forecasting wave conditions for seas around the UK and Scotland, and serve as a tool for supplying boundary hydrodynamic parameters for small scale regional wave and tidal models. Further, this wave model, when run for longer time periods, would supply wave conditions to estimate site specific extreme wave parameters for device designs and assessing survivability limits. Moreover, this model can provide site specific wave parameters for assessing environmental impact (eg., sediment transport change patterns) and ecological consequences of energy extraction.

2. Wave model overview

The spectral wave module from MIKE 21 suite [20] has been selected for the simulation of waves and it is a widely used numerical tool by both the scientific community and industry worldwide. The model simulates the growth, decay and transformation of wind-generated sea and swells in offshore and coastal areas. This model accounts for the wave growth by the action of wind, non-linear wave-wave interaction, dissipation of energy due to white-capping, bottom friction and depth-induced wave breaking, refraction and shoaling, wave-current interaction and the effect of time-varying water depth. A cell-centred finite volume method is applied in the discretization of the governing equations in geographical and spectral space and a multi-sequence explicit method is applied for the wave propagation with the time integration carried out using a fractional step approach. This model produces phase averaged wave parameters as output for the computational area.

The wind waves are expressed by the wave action density spectrum $N(\sigma,\theta)$, where σ is the relative (intrinsic) angular frequency and θ is the direction of wave propagation. The relative angular frequency can be related to the absolute angular frequency (ω) by the linear dispersion relationship as,

$$\sigma = \sqrt{gk \tanh(kd)} = \omega - \bar{k} \cdot \bar{U} \quad (1)$$

where, g is gravity constant; k is wave number; d is water depth; $\bar{U}$ is current velocity vector and $\bar{k}$ is wave number vector with magnitude k and direction θ.

MIKE 21 spectral wave model includes two methods of wave simulation namely, (i) the directional decoupled parametric formulation and (ii) the fully spectral formulation, both based on the wave action conservation equations in either Cartesian (for small scale applications) or spherical (for large scale applications) co-ordinate systems (Komen at al, [21], Young, [22]). The first formulation is based on a parameterisation of zeroth and first order moment of the wave action spectrum as dependent variables, whereas the second formulation involves the directional frequency wave action spectrum as the dependent variable.

The wave action density spectrum $N(\sigma,\theta)$ can be related to the energy density $E(\sigma,\theta)$ by the relation

$$N(\sigma,\theta) = \frac{E(\sigma,\theta)}{\sigma} \quad (2)$$

In the fully spectral formulation, the governing equation is the wave action balance equation. The conservation equations for wave action in Cartesian co-ordinates is given by

$$\frac{\partial N}{\partial t} + \nabla \cdot (\overline{v} N) = \frac{S}{\sigma} \tag{3}$$

where, $N(\overline{x}, \sigma, \theta, t)$ is the action density, t is the time, $\overline{v} = (c_x, c_y, c_{\sigma,} c_\theta)$ is the propagation velocity (as expressed in eqns 4-6) of a wave group in the four dimensional phase space, $\overline{x}, \sigma$, θ & t, ∇ is the four-dimensional differential operator and S is the source term for energy balance equation. The wave group propagation velocities $c_x, c_y, c_{\sigma,} c_\theta$ in four-dimensional phase space are:

$$\left(c_{x,} c_y\right) = \frac{d\overline{x}}{dt} = \overline{c_g} + \overline{U} = \frac{1}{2}\left(1 + \frac{2kd}{sinh\left(2kd\right)}\right)\frac{\sigma}{k} + \overline{U} \tag{4}$$

$$c_\sigma = \frac{d\sigma}{dt} = \frac{\partial \sigma}{\partial d}\left[\frac{\partial d}{\partial t} + \overline{U} \cdot \nabla_{\overline{x}} d\right] - c_g \overline{k} \cdot \frac{\partial \overline{U}}{\partial s} \tag{5}$$

$$c_\theta = \frac{d\theta}{dt} = -\frac{1}{k}\left[\frac{\partial \sigma}{\partial d}\frac{\partial d}{\partial m} + \overline{k} \cdot \frac{\partial \overline{U}}{\partial m}\right] \tag{6}$$

where, $\nabla_{\overline{x}}$ is the two dimensional differential operator in the $\overline{x}$ space, $\overline{x} = \left(x, y\right)$ is the Cartesian co-ordinates, s is the space co-ordinate in wave direction θ, and m is the co-ordinate perpendicular to s. The source function term S is given by

$$S = S_{in} + S_{nl} + S_{ds} + S_{bot} + S_{surf} \tag{7}$$

where, S_{in} is the momentum transfer of wind energy to the wave generation; S_{nl} is the energy transfer due to non-linear wave –wave interaction; S_{ds} is the energy dissipation of wave energy due to white-capping; S_{bot} is the energy dissipation due to bottom friction; S_{surf} is the energy dissipation due to depth-induced breaking.

The source functions S_{in}, S_{nl} and S_{ds} are similar to WAM Cycle 4 model (Komen et al., [21], WAMDI Group [18] and the wind input is based on Janssen's [23-24] quasi-linear theory. Further details can be found in [20].

3. Model set-up

3.1 Bathymetry and mesh generation

An unstructured computational mesh (see Figure 2) was constructed using MIKE 21 mesh generator and this covered the North Atlantic region 10^{o}E – 75^{o}W and 10^{o}N-70^{o}N. It is well known fact that swells generated in the Atlantic Ocean travels a long way to reach Scottish waters, and they tend to carry higher energy which is highly beneficial to wave energy community. As the objective was to capture long distance swells propagating towards the UK, although it takes up high computing resources, this had been the reason for selecting such a large computational domain. The sea water depth data compiled from the sources, GEBCO [25] and Marine Scotland [26] have been used to generate the bathymetry within the computational domain as can be seen in Figure 2. The grid resolution of the GEBCO bathymetry data was 30 arc seconds, which was used for most of the model domain except for Orkney, Pentland Firth, Shetland and north-west coast of Lewis regions which were covered by the Marine Scotland's measured bathymetry data. The size of both GEBCO and Marine Scotland data sets were too large for the MIKE 21 mesh generator to manage at one time, hence a data filter had been applied with the purpose to reduce the data size but without losing data integrity, which resulted in the size of the spatial grids reduced to 100 m (Easting) x 100 m (Northing) for the entire Orkney and Pentland waters and device deployment locations around it, and also along the coast in the north. For the rest of the UK, Ireland and English Channel, about 2 km x 2 km grid data resolution was selected. In the Icelandic and Faroe Islands regions about 5 km x 5 km, in the North Sea 3 km x 6 km, and for the rest of the North Atlantic deep water locations 10 km x 10 km spacing were used.

For triangulation of unstructured mesh the 'Natural neighbour' interpolation method [20], which is a geometric estimation technique that uses natural neighbourhood regions generated around each point in the data set and suitable for dealing with a variety of spatial data themes with clustered or highly linear distributions, has been selected. In total 71,793 elements with various mesh resolutions have been produced for the entire computational domain as shown in Figure 2. Highly finer mesh resolutions with a mesh area of 0.0005 square degrees for Orkney and Pentland waters, 0.001 square degrees for the Hebrides and North West regions of Scotland (see Figure 3) and 0.75 square degrees for North Atlantic Ocean were used. Such a high resolution in the mesh was necessary for describing the shallow water hydrodynamics within the model; and also for providing input boundary conditions if another small scale model is involved. One such exercise for a 3-dimensional combined wave and tidal flow model, which was separately constructed for the Terawatt project, can be seen in Venugopal and Nemalidinne [27].

3.2 Model forcing and physical processes

The model was forced with 10 m level U- and V- wind speed data obtained from the operational products of the European Centre for Medium-Range Weather Forecasts (ECMWF [28]) at 6 hrs interval with a spatial resolution of 0.125^o x 0.125^o. The model was run in 'fully spectral' mode as briefed in section 2 above, with 'Instationary formulation'. The 'coupled' type of air-sea interaction has been chosen for the wind boundary input with a Charnock parameter of 0.01. According to the coupled model, the sea roughness, z_o is given by [20]

$$z_o = \frac{z_{charnock} u_*^2}{g} \left(1 - \frac{\tau_w}{\rho_{air} u_*^2} \right)^{-1/2} \quad (8)$$

where, $z_{charnock}$ is the Charnock parameter, u_* is the friction velocity which was calculated by Janssen [24] by assuming a logarithmic profile for wind speed, the τ_w is the wave induced stress, ρ_{air} is the density of air and g is the gravity constant.

The fully spectral formulation is a computationally expense technique, however when the model is forced with wind input, it ensures fetch unlimited wave growth, decay and transformation of wind sea and swells. The number of frequencies used for the model were 25 with f_{min}=0.04 Hz. The frequency factor was 1.1 and a logarithmic distribution of frequencies was generated. The directional discretisation had 24 directional bins, each with 15^o resolution, with 360 degree wave coverage.

No current, ice coverage and diffraction were included into the model as this would further increase computational efforts and also as it can be seen later that without including these additional inputs, a successful calibration was achieved. Dissipation due to whitecapping, bottom friction and depth-induced wave breaking were considered in the simulations and the energy transfer was activated. A quadruplet-wave interaction has been applied. A low order fast algorithm has been chosen as the solution technique with the 'maximum number of levels in transport calculation' as 32. The source function describing the dissipation due to white-capping was based on the theory of Hasselmann [29] and Komen et al., [21]. The values applied for *Cdis* and *DELTAdis* (δ) were 2 and 0.8 respectively, which were also incidentally found to be close to the values suggested by Bidlot et al., [30], who revised the whitecapping formulation proposed by Komen et al., [21], for combined wind sea and swell generation conditions. Bottom friction was considered according to *Nikuradse roughness* (Weber, [31]) and the value applied was 0.04 m. The formulation for wave breaking was based on breaking model specified gamma (Nelson, [32-33], Ruessink et al., [34]). The *gamma* and *alpha* values were applied as 0.8 and 1 respectively. For detailed description of the above source terms refer to MIKE21 SW manual [20]. The process of selection of model parameters values is further discussed in section 5.1 below.

The integral wave parameters such as significant wave height, peak wave period, mean wave period, energy period, peak wave direction, mean wave direction, directional standard deviation, and wave power have been resolved for every 30 minutes as point series and for every 6 hours as area (contour) series.

4. Wave data sources for model calibration and validation

Measured wave data from wave buoys deployed around Scotland have been utilised for model's calibration and validation. Details of their names, locations and duration of the data are listed in Table 1. The locations of the buoys are shown in Figure 4. The Cefas, Blackstone, Moray Firth and Firth of Forth buoys data are in public domain from the WaveNet [35]. The Bragar buoy has been deployed for the Hebridean Marine Energy Futures project (Vogler and Venugopal, [36]) and the data are not in public domain yet; for this reason though this wave data were used for model calibration and validation, the results discussed in section 5 will not include Bragar data. The time series of significant wave height (H_{m0}), peak wave period (T_P) and peak wave direction (Dir_P) were only accessible from the public domain buoy data. While it is possible to resolve various wave parameters including wave power from MIKE21 model, only the above wave parameters available from wave buoys have been selected for calibration and validation.

5. Results and Discussion

5.1 Calibration of the wave model

The wave conditions hindcast for May 2012 for Cefas, Blackstone, Moray Firth and Firth of Forth are shown in Figures 5-8 respectively. All four wave measurement's summary statistics have been stored at 30 minutes interval by Wavenet [35] and hence the model output parameters have also been extracted at corresponding time stamps. Note that the wave buoy denoted as Orkney-E in Figure 4 is also privately owned and the data was not accessible at the calibration stage. Usually at the calibration stage, the primary task is to match the model output parameters with measured wave parameters, by tuning those model input parameters that account for source functions given in Eqn. (7). The input parameters which may need tuning include bottom friction, wave breaking parameters, whitecapping, wind, current and water level data, mesh resolution and input boundary. For the current work, during the model calibration stage, initially it was decided to carry out the hindcasting with model's default values describing whitecapping, bottom friction and wave breaking, and this has produced values significantly different from the measurements. As there is no single methodology exists in selecting a set of optimised values of the tuneable input parameters to describe the relevant physical processes, it was decided to attempt a trial and error approach. This involved running the model for a number of cases with various combinations of parameter values, yet keeping the values within the range recommended in the literature as provided in [20]. As an example, when the whitecapping coefficient, *Cdis*, which control the rate of white-cap dissipation, was changed to 3.0 from its default value of 4.5 and another control parameter δ was kept at its default value of 0.5, and at the same time keeping the wave breaking parameter $\gamma = 0.8$ and $\alpha = 1.0$ and bottom friction (represented by the Nikuradse roughness), $kn = 0.04$ m, has produced significantly larger wave heights than measurements. The same combination but with *Cdis* = 1.5 has produced small wave heights than measurements, and at the same time, hindcast peak wave periods were slightly higher than measurements. Finally, the values mentioned above in section 3.2 were found to be producing an overall good agreement with measured H_{m0}, T_P and Dir_P which were finally adopted for further calibration and validation.

As illustrated in Figures 5-8, the comparison of hindcast significant wave height from model has resulted in an excellent agreement with measured significant wave heights for all four sites. Also, with the exception of few time periods, in general, a very good comparison was found for peak wave periods and peak wave directions for all four sites. This is a known fact that trying to correlate peak wave periods or peak wave directions from model with measurements may produce significant discrepancies in contrast to mean wave periods and mean wave directions. However, these latter two parameters were not available from none of the buoy measurements to compare with. Also it is worth noting that there were significant differences between the model and measurements for up to the first 3 days for all sites, and this was due to the model initiating from a cold start where a fully developed sea condition might not have yet been reached. Nevertheless, referring to Table 2, the quality parameters calculated for four sites [eg., for significant wave height: Bias is in the range -0.09 to +0.11 m, Root Mean Square Error, RMSE is in the range 0.23 – 0.40 m, Scatter Index in the range 0.21 – 0.28), for peak wave period (Bias: -0.38 to +0.29 s, RMSE: 1.62 – 2.76 s, Scatter Index: 0.17 – 0.39)] clearly illustrates that the hindcast model performed well. The definitions for quality indices are given through Eqns (9)-(14). For peak wave direction the quality indices are relatively poor, yet they are considered satisfactory. One must also bear in mind that for the above quality indices calculations, the time series for the whole month was used without avoiding the model initial ramp up period of 3 or 4 days, which could have influenced the statistics as well. The Pearsons's correlation coefficients, *R* - values calculated, for example for wave heights, ranged from 0.88 to 0.97 which indicates the calibration for significant wave height was highly accurate.

$$Bias = \frac{1}{N}\sum_{i=1}^{N}\left(x_{o_i} - x_{m_i}\right) \tag{9}$$

$$RMSE = \sqrt{\frac{1}{N}\sum_{i=1}^{N}\left(x_{m_i} - x_{o_i}\right)^2} \tag{10}$$

$$SI = \frac{RMSE}{\overline{x}_o} \tag{11}$$

$$\overline{x}_o = \frac{1}{N}\sum_{i=1}^{N}\left(x_{o_i}\right) \tag{12}$$

$$\overline{x}_m = \frac{1}{N}\sum_{i=1}^{N}\left(x_{m_i}\right) \tag{13}$$

$$R = \frac{\sum_{i=1}^{N}\left(x_{o_i} - \overline{x}_o\right)\left(x_{m_i} - \overline{x}_m\right)}{\sqrt{\sum_{i=1}^{N}\left(x_{o_i} - \overline{x}_o\right)^2\left(x_{m_i} - \overline{x}_m\right)^2}} \tag{14}$$

where, x_o is the observed (field) data and x_m is the model data.

5.2 Validation of the wave model

With sufficient confidence built up on the calibration of the model as described above, as next step, an attempt to validate the model for different time periods have been undertaken. Although the model validation has been performed for different time periods (i.e., Oct-2011, Jan-2012, March-2012, see Table 1.), considering space limitations the time series for October 2011 are only shown in Figures 9-12 for four sites. The performance indices (or quality parameters) calculated for Cefas, Blackstone, Moray Firth and Firth of Forth for Oct-2011, Jan-2012 and

March-2012 are listed in Tables 3 – 5 respectively. As indicated by the quality parameters, an excellent agreement has been noticed for significant wave height, however for Moray Firth, some discrepancies in peak wave period and direction are seen. Also for Moray Firth and Firth of Forth, sudden changes in wave directions are distinct and while the model captured this better for Firth of Forth, resolving the same parameter for Moray Firth has not been perfect.

5.3 Wave Hindcasting

As previously discussed, the key objective of setting up this model is to assess wave power resources for potential device deployment locations around Orkney and to provide boundary conditions for running regional/small scale wave and tidal flow models within the TeraWatt project. The time duration considered for calibration and validation processes in the above sections were relatively small as only monthly hindcasting have been undertaken. In the assessment of the impact of energy extraction (this could be accomplished by including an individual or array of energy extraction devices into the wave model directly or can be inferred from another hydrodynamic software or CFD methods and eventually be linked with MIKE21) on morphological, ecological and other environmental changes, a longer term data would usually be required. It would then create an interest to learn about how well the wave model is able to hindcast longer term data. With this in mind, the model simulation was carried out for the year 2010 for which wave measurement data for Blackstone, Cefas, Orkney-E, Moray Firth and Firth of Forth were available and the results are presented in Figures 13 to 17 respectively. These results generally indicate that the hindcasting of wave parameters, particularly the significant wave height, for all five sites agreed well with the measurements for most of the time periods. As the hindcasting data covered both summer and winter months, it is evident that the model was able to resolve wave conditions for different seasons of a year.

Inspection of individual locations reveals some interesting features; for Blackstone (Figure 13), the peaks in the significant wave height time series are mostly captured by the model, however, it appears though the highest peak that occurred in November has been under-predicted. A good agreement in peak periods and peak wave directions is encouraging. A similar observation for Cefas location was noticed as seen in Figure 14, however, for a considerable period from mid of September to mid of November, there were no data recorded by the Cefas buoy, yet the model appear to provide the missing wave height, period and direction data and fills this gap in the measurement. The authors believe that this ‘filling data’ could be as accurate as the real measured data as the model data joins and fits in well with measured data for time periods where the buoy data was missing. This is further confirmed by a similar trend in the variation of wave parameters recorded at the Blackstone site in Figure 13, as the two measurement locations are close by and it could be possible that the wave growth and propagation could have related patterns.

The results presented in Figure 15 are for the Orkney-E location where the wave buoy data for the year 2010 has been provided by the European Marine Energy Centre. Note that the location has not been previously used as a calibration site; nonetheless, the excellent comparison seen in Figure 15 indicates that the model indeed performed well for un-calibrated regions as well. Similar to Cefas location, Orkney-E buoy also had missing data and evidently the model data was found to be filling this gap and linking well with the measured data wherever the data were missing. Another observation in Figure 15 is that the buoy measurements appear to have spurious data, eg., large significant wave height in December and large wave periods of magnitude about 40 seconds in June and December, that are not seen in the model results, which again confirms that the model data could be considered as a substitute for unreliable or erratic measurements.

The model predictions are compared with measurements for Moray Firth and Firth of Forth in Figures 16 and 17 respectively. Note that these two locations are in the North Sea. For both locations the significant wave height produced a very good correlation with measured data. While the comparison of peak wave period and peak wave direction for Firth of Forth agreed better, for Moray Firth site, some considerable difference in T_p with model data was observed, in comparison to Blackstone, Cefas and Orkney-E sites. It appears that for both these North Sea sites, the significant wave height for majority of the time period in the year 2010 is less than 2 m and yet the model was able to predict this accurately. Looking at the peak periods, although the hindcast values are within the bound of measurements, they are often quite variable. The wave heights appear to be about less than 1m for most of the time for the months from April to August, however the corresponding wave periods varies from about 3 to 12 s indicating that some of the long period waves carried far less energy from North Sea.

Moreover, a glance at the peak wave direction shows that most of the time the waves have travelled from North East (about 30 deg from due North) to East (90 deg), and as Shetland lies in its path, the island would have acted as a barrier altering the wave propagation, however it is difficult to confirm this without further study. Further, in the peak direction plot, many single vertical lines in the measured data can be seen and these are corresponding to only one single point deviating abruptly from the 'expected' peak wave direction, i.e., a sudden change of wave direction, say from 90 deg to 270 deg and back to 90 deg within 30 minutes is not normal. As this behaviour occurred many times in the measured data, this may make the measured wave direction not credible. The another reason for the discrepancy could be that the model was run without accounting for shallow water triad-wave energy transfer and currents, particularly, the strong tidal currents (see Venugopal and Nemalidinne [27]) that occurs in the Pentland Firth, plus any likelihood occurrence of wave diffraction around the north east tip of Scottish mainland, which would have had some impact on the wave propagation and modification; however realising the good correlation with significant wave height, it is difficult to pinpoint the sources responsible at this stage. While a nearly similar observation is noticed for Firth of Forth in Figure 17, however the model agreed relatively better for this location than Moray Firth. Perhaps, if one trusts that the Shetland indeed obstructed the wave, it may then be reasonable to believe that the Firth of Forth was less influenced by this island, as this is not directly in the downstream when waves propagate in the 30-90 deg sector.

The another way of inspecting the model results is to represent the data as scatter plots as shown in Figures 18-20 for three locations. The results are also listed in Table 5 as quality index parameters for all five sites under investigation. For all three sites (Figures 18-20), the data for significant wave height from model and measurement are found to be in close proximity to or on the equality line illustrating that the significant wave heights were highly accurately resolved, which is also indicated by values of low Bias (-0.10 to +0.27 m), low RMSE (0.25 to 0.45m), low Scatter Index (0.19 to 0.3) and very high correlation coefficient above 0.94 in Table 5. For peak wave period, except the Moray Firth site, the correlation coefficient is found to be above 0.64 and low values of Bias, RMSE and Scatter index are obtained. For peak wave direction, the correlation is lower than wave height and wave period, however their correlation coefficients, except Moray Firth, are found to be above 0.57. This low value can be explained by re-visiting correlation plots for peak wave direction, in that, the large scatter is attributed to the way in which the wave direction is represented; for example, a measured direction of 0.0 deg and model produced direction of 360 deg are literally the same, however when this is represented as a scatter plot they would produce ‘zero’ correlation and the same applicable to any other values close to 0.0 deg or 360 deg, thus yielding a large scatter and incorrect correlation values.

In addition to the above sites, three relatively shallow water locations have also been considered for inspection of wave conditions produced by the MIKE21 model, and the results are shown in Figures 21 and 22, for significant wave heights and mean wave directions respectively for the year 2010. Noting that these shallow water locations have been randomly selected at which no measured data were available to compare with the model outputs, it was decided to use another numerical wave model’s results for verification. In order to perform this, wave data have been downloaded from the ECMWF wave model archives which were produced using the WAM model [18]. The downside of it is, the type of access the authors have with the ECMWF wave data, allows only to download gridded data stored at a minimum grid spacing of 0.125 deg x 0.125 deg resolution, which pose a problem when matching with a chosen shallow water location to the ECMWF grids; however, the authors have made an attempt and selected three locations where the water depth was shallow and the ECMWF data was available. These are denoted as Isle of Lewis (58.375^{o}N, 6.625^{o}W, water depth, d = 16.6 m), Westray (59.25^{o}N, 3.0^{o}W, d = 13.75 m) and Dornoch (57.875^{o}N, 3.875^{o}W, d = 11.0 m) in Figure 4.

Note that in Figures 21 and 22, it was not possible to compare wave periods, as the wave period stored in the present wave model (i.e., mean wave period) was different from the wave period (i.e., energy wave period) available for download from the ECMWF. Considering the time it will consume to re-run the present model to produce energy wave period, this idea was not pursued.

It is evident that for Isle of Lewis (correlation coefficient R = 0.95, SI = 0.19 and Bias = 0.13) and Dornoch (R = 0.9, SI = 0.45, Bias = 0.17) sites, the significant wave height obtained from the present model matched very well with ECWMF model, however, for the Westray site some significant differences (R = 0.53, SI = 0.57 and Bias = -0.27) were noticed. In addition, for the Westray site, the value of the significant wave height obtained from the ECMWF model in December is over 9 m, which makes one to wonder the likelihood of such a large magnitude wave events to occur in a 13.75 m water depth!

In the case of mean wave direction (Figure 22), it appears that the MIKE21 model provides a consistent (refer to Figure 15 for Orkney site), less scattered values throughout the time period considered, whereas the WAM model's wave direction often rapidly changes its course. Considering the fact that these results are both from numerical models, it would be difficult to take side as to which model is accurate for these shallow water locations; nevertheless based on the results obtained, the MIKE21 model, can be applied for resource assessment in shallow water conditions.

5.4 Comparison of significant wave height and wave power with UK Marine Atlas

In the above sections, wave model calibration, validation and hindcasting have been presented for single point locations, and in this section, in particular, the significant wave height and wave power are presented as contour maps for a region that comprise the boundaries roughly representing the Scottish waters. Figures 23 and 24 show the contour maps of the statistical mean and maximum significant wave height derived for the whole year 2010 and these plots illustrate the spatial variation of significant wave height for different locations. Referring to Figure 1, for the locations west of Orkney mainland where wave device deployment activities are planned (noted by yellow colour rectangular boxes), the annual mean significant wave height (refer Figure 23) is observed to be about 1.75 to 2.0 m and the maximum significant wave height is found to be about 7 to 8 m. Further, it is encouraging to note that the annual mean significant wave height reported from the 'enhanced model' (ABPMer Report, [37], see Figure 25) in the Atlas of UK Marine Renewable Energy Resources (ABPMer, [19]) for the same location is found to be 2.01 to 2.25 m which is very close to the one year average found from the present work. While the UK Marine Atlas was calculated based on a hindcasting of the average of 7 years data (1 June 2000 to 31 May 2007), the enhanced model, which mainly covered Orkney and Pentland Firth (region marked by thick black line in Figure 25), results were based on a 20 year (1 Jan 1990 to 31 Dec 2009) hindcast. Also the Figure 25 itself an obvious explanation of the need for setting up another refined wave model, such as the present work, as in the UK Marine Atlas, the values appeared to be based on a course mesh (for regions other than the enhanced model), in which the variation of wave heights are represented by rectangles of constant values for a large area which may not be realistic.

The wave energy flux or wave power (P) in a sea state transported at any water depth can be calculated as

$$P = \rho g \int_0^{2\pi} \int_0^{\infty} S(f,\theta)\, \bar{C}_g(f,\theta)\; df d\theta \qquad (15)$$

where, $S(f,\theta)$ is the directional energy spectral density at frequency f and wave propagation angle θ, and $\bar{C}_g(f,\theta)$ is the resultant wave group velocity ([20]).

The wave power calculated using Eqn (15) at point locations corresponding to Cefas, Blackstone, Orkney, Moray Firth and Firth of Forth are shown in Figures 26(a) and(b) for the year 2010. In Figure 26(b), the power scale axis has been limited at 50 kW/m for Cefas, Blackstone, Orkney sites and 20 kW/m for Moray Firth and Firth of Forth sites, for better visualisation at these limited levels. This figure demonstrates, as expected, that the wave power during the winter months is very high, reaching over 600 kW/m for Cefas and Blackstone sites. For the Orkney-E site, a value of about 300 kW/m is obtained for Dec 2010. Lower values of wave power are observed for Firth of Forth and Moray Firth, making these sites not a candidate for wave power developments.

The statistical mean and maximum wave power calculated for the same region as in Figures 23 and 24, are shown in Figures 27 and 28 as contour plots. From [37], the contour lines (not shown here) representing the annual mean wave power for Orkney wave power strategic regions, indicate values from 30-40 kW/m which was based on 20 year hindcast by the enhanced model as mentioned above. This value is however, comparable to the one obtained from the present model which has produced a value in the range about 25 to 35 kW/m, thus increasing the confidence in using the present model for wave power calculations.

Additionally, the wave power rose diagram plotted in Figure 29, depicts the proportion of the wave power with respect to wave propagation direction for the year 2010. The data have been worked out using wave power computed for every 30 min blocks for the whole year. Each division of the x and y axis represents a fraction of 5% level. The circle marked with white colour indicates the fraction of the wave power resource which is less than 5 kW/m. It is clear from this plot that for Moray Firth and Firth of Forth about 70 to 73% of wave power is less than 5 kW/m, whereas, for the Orkney-E site only 22.5% are found to be less than 5 kW/m and the most probable wave direction appears to be form due West. For the Blackstone and Cefas sites, wave power values over 105 kW/m have been hindcast and the majority of the waves appear to be propagating from South-West direction, and only about 3 to 9 % of wave power are less than 5 kW/m.

It becomes clear that the model hindcast needs to be carried out for longer time period as done in [37], if the aim is to estimate statistically consistent wave resources. Considering the limited computational resources, it was not possible to execute the model for such a long period of hindcasting for the present work, however, having built up the confidence, the future work will include extended periods with the inclusion of tidal currents and other relevant hydrodynamic processes. Despite the wave model results are based on one year hindcast, it is evident from the plots, tables and arguments presented above that the model performed well and could be adopted for reliable hindcasting and even forecasting of wave conditions and wave power for regions in question.

6. Conclusions

A large scale wave model, comprising North Atlantic Ocean bounded by latitudes 10^{o} N - 70^{o} N and longitudes 10^{o} E-75^{o} W, has been developed using the state-of-art MIKE21 suite for hindcasting of wave parameters and wave power. The model included finer scale bathymetry and gird resolutions around Scotland, specifically to the Orkney and Pentland Waters, where wave and tidal energy device deployment activities are consented by the Crown Estate. The model was forced by the wind data obtained from European Centre for Medium Range Weather Forecasts (EWCMWF) at 0.125 deg resolution. The methodology behind the processing of bathymetry, mesh construction and selection of model input parameters which account for source terms and energy transfer have been described. A comprehensive model calibration and validation has been conducted for four sites, Cefas and Blackstone in the North Atlantic Ocean, and, Moray Firth and Firth of Forth in the North Sea. In addition, a one-year hindcasting has been undertaken.

The wave hindcasting for the year 2010 has successfully reproduced significant wave heights for Cefas, Blackstone, Orkney-E, Moray Firth and Firth of Forth sites with correlation coefficients higher than 0.96. The peak wave periods for Cefas, Blackstone, Orkney-E sites were found to be well in agreement with buoy measurements with correlation coefficients above 0.69, however, for Moray Firth and Firth of Forth significant differences between model and measured values noted by less marked correlation coefficients of 0.39 and 0.64 respectively. The impact of tidal currents, wave diffraction and triad wave interactions have not been considered in the present model, doing so may have improved the results for Moray Firth and Firth of Forth, which however needs further work. The annual mean significant wave height and wave power obtained for Orkney strategic wave power deployment sites based on one-year wave hindcast were found to be close to the values reported in the Atlas of UK Marine Renewable Energy Resources.

The results of the study illustrated that the wave model could be employed with high level of confidence for wave hindcasting and even forecasting of various wave parameters and wave power, in particular, for Orkney and Pentland Firth waters and Outer Hebrides.

Acknowledgments

The authors are grateful for the financial support of the UK Engineering and Physical Sciences Research Council (EPSRC) through the Terawatt-Large scale Interactive coupled 3D modelling for wave and tidal energy resource and environmental impact consortium. The authors are also grateful to Cefas (UK) for wave buoys data, European Centre for Medium-Range Weather Forecasts (ECMWF) for providing wind data, European Marine Energy Centre (EMEC) for providing wave buoy data for Orkney and for Marine Scotland Sciences for providing bathymetry data.

References

[1] renews. http://renews.biz/special-reports/, 2014; accessed on 22/07/14.

[2] The Crown Estate. UK wave and tidal key resource areas project. Technical report, http://www.thecrownestate.co.uk/energy-infrastructure/wave-and-tidal/pentland-firth-and-orkney-waters/enabling-actions/projects-and-publications/, Oct 2012; accessed on 28/05/14.

[3] Aquamarine Power. http://www.aquamarinepower.com/projects, accessed on 28/05/14.

[4] Pelamis wave power. http://www.pelamiswave.com/our-projects/project/2/ScottishPower-Renewables-at-EMEC, accessed on 28/05/14.

[5] Alstom. http://www.alstom.com/power/renewables/ocean-energy/, accessed on 28/05/14.

[6] Andritz Hydro Hammerfest. http://www.hammerfeststrom.com/, accessed on 28/05/14.

[7] AW Energy. http://aw-energy.com/, accessed on 28/05/14.

[8] Voith Hydro. http://voith.com/en/products-services/hydro-power/ocean-energies-587.html, accessed on 28/05/14.

[9] Wello Oy. http://www.wello.eu/penguin.php, accessed on 28/05/14.

[10] http://www.emec.org.uk/about-us/our-tidal-clients/, accessed on 28/05/14.

[11] http://www.emec.org.uk/about-us/wave-clients/ , accessed on 28/05/14.

[12] http://www.scotland.gov.uk/Topics/marine/marineenergy, accessed on 28/05/14.

[13] Swail VR, Cardone VJ, Cox AT. A long term North Atlantic wave hindcast. In: 5th International Workshop on Wave Hindcasting and Forecasting, January 26-30, Melbourne, Florida, 1998.

[14] Swail VR, Ceccacci EA, Cox AT. The AES40 North Atlantic wave reanalysis: validation and climate assessment. In: 6th International Workshop On Wave Hindcasting and Forecasting, November 6-10, Monterey, California, USA, 2000.

[15] Dodet G, Bertin X, Taborda, R. Wave climate variability in the North-East Atlantic Ocean over the last six decades. Ocean Modelling 2010; 31: 120–131.

[16] Tolman HL. 2009. User manual and system documentation of WAVEWATCH III version 3.14. NOAA/NWS/NCEP/MMAB Technical Note 276, 2009; 194 p.

[17] Galanis G, Chu PC, Kallos G, Kuo Y-H, Dodson CTJ. Wave height characteristics in the north Atlantic ocean: a new approach based on statistical and geometrical techniques. Stochastic Environmental Research and Risk Assessment 2012; 26(1): 83-103.

[18] WAMDI Group. The WAM model—A third generation ocean wave prediction model. J. Phys. Oceanogr., 1988; 18: 1775–1810.

[19] ABPmer. Atlas of UK Marine Renewable Energy Resources. http://www.renewables-atlas.info; 2008. Date of access 07 July 2014.

[20] MIKE 21. Wave Modelling User guide, Scientific Document, Danish Hydraulic Institute, Denmark; 2012.

[21] Komen GJ, Cavaleri L, Donelan M, Hasselmann K, Hasselmann S, Janssen PAEM. Dynamics and Modelling of Ocean Waves. Cambridge Univ. Press, New York; 1994, 532.

[22] Young IR. Wind generated ocean waves. Elsevier Ocean Engineering Book Series, Vol 2, Eds. Bhattacharyya, R and McCormick, M.E, ISBN: 978-0-08-043317-2; 1999.

[23] Janssen PAEM. Wave induced stress and the drag of airflow over sea waves, J. Phys. Oceanogr. 1989; 19: 745-754.

[24] Janssen PAEM. Quasi-linear theory of wind wave generation applied to wave forecasting, J. Phys. Oceanogr. 1991; 21: 1631-1642.

[25] GEBCO. http://www.gebco.net/ ; accessed on 28/05/14.

[26] Marine Scotland. http://www.scotland.gov.uk/Topics/marine/science/MSInteractive/datatype/Bathymetry/data. accessed on 28/05/14.

[27] Venugopal V, Nemalidinne R. Marine energy resource assessment for Orkney and Pentland waters with a coupled wave and tidal flow. In: Proceedings of the 33th International Conference on Ocean, Offshore and Arctic Engineering OMAE2014, June 8-13, 2014, San Francisco, AC, USA, paper no OMAE2014-24027, 2014.

[28] ECMWF. http://www.ecmwf.int/; accessed on 28/05/14.

[29] Hasselmann K. On the spectral dissipation of ocean waves due to whitecapping, Bound. Layer Meteor. 1974; 6: 107-127.

[30] Bidlot J, Janssen P, Abdalla S. A revised formulation of ocean wave dissipation and its model impact. Technical Report Memorandum 509, ECMWF, Reading, UK; 2007.

[31] Weber SL. Bottom friction for wind sea and swell in extreme depth-limited situations, J. Phys. Oceanogr. 1991; 21: 149-172.

[32] Nelson RC. Design wave heights on very mild slopes: An experimental study, Civil. Eng. Trans., Inst. Eng. 1987; 29: 157-161.

[33] Nelson RC. Depth limited wave heights in very flat regions. Coastal Eng. 1994; 23: 43-59.

[34] Ruessink BG, Walstra DJR, Southgate H.N. Calibration and verification of a parametric wave model on barred beaches. Coastal Eng. 2003; 48: 139-149.

[35] WaveNet. http://www.cefas.defra.gov.uk/our-science/observing-and-modelling/monitoring-programmes/wavenet.aspx; accessed on 28/05/14.

[36] Vogler A, Venugopal V. Hebridean marine energy resources: wave power characterisation using a buoy network. In: Proceedings of 31th International Conference on Offshore Mechanics and Arctic Engineering, OMAE2012, Rio de Janeiro, Brazil, OMAE2012-83658, 2012.

[37] APBMer. Report R.1936, Unpublished, 2012.

Tables

Table 1. Details of buoy data used for model calibration and validation

Process	Buoys/site name	Latitude	Longitude	Water depth (m)	Time period
Calibration	Cefas	57.292333° N	7.914333° W	100	May 2012
	Blackstone	56.062000° N	7.056833° W	97	May 2012
	Moray Firth	57.966333° N	3.333167° W	54	May 2012
	Firth of Forth	56.188167° N	2.503833° W	65	May 2012
Validation	Cefas	57.292333° N	7.914333° W	100	Oct 2011, Jan 2012,Mar 2012
	Blackstone	56.062000° N	7.056833° W	97	Oct 2011, Jan 2012,Mar 2012
	Orkney E	58.970200° N	3.390900° W	53	-
	Moray Firth	57.966333° N	3.333167° W	54	Oct 2011, Jan 2012,Mar 2012
	Firth of Forth	56.188167° N	2.503833° W	65	Oct 2011, Jan 2012,Mar 2012

Table 2. Quality Indices-May 2012

Site	Wave parameters	Mean	Bias	RMSE	Bias/Mean	SI	R
Cefas	Hm0 (m)	1.88	0.11	0.40	0.06	0.21	0.96
	Tp (s)	9.30	0.01	1.62	0.00	0.17	0.69
	Dirp (deg)	216.77	-33.78	148.58	-0.16	0.69	0.45
Blackstone	Hm0 (m)	1.50	0.05	0.31	0.03	0.21	0.97
	Tp (s)	8.57	0.29	2.30	0.03	0.27	0.60
	Dirp (deg)	291.00	-20.40	60.35	-0.07	0.21	0.27
Moray Forth	Hm0 (m)	0.91	-0.15	0.26	-0.17	0.28	0.88
	Tp (s)	7.08	-0.33	2.76	-0.05	0.39	0.45
	Dirp (deg)	79.86	-15.24	64.46	-0.19	0.81	0.36
Firth of Forth	Hm0 (m)	0.97	-0.09	0.23	-0.09	0.24	0.88
	Tp (s)	6.97	-0.38	2.08	-0.05	0.30	0.40
	Dirp (deg)	71.26	-4.57	33.37	-0.06	0.47	0.78

Table 3. Quality indices for October 2011

Site	Wave parameters	Mean	Bias	RMSE	Bias/Mean	SI	R
Cefas	Hm0 (m)	3.25	0.44	0.79	0.13	0.24	0.90
	Tp (s)	11.32	0.01	1.83	0.00	0.16	0.74
	Dirp (deg)	272.50	-14.06	31.01	-0.05	0.11	0.68
Blackstone	Hm0 (m)	3.25	-0.06	0.46	-0.22	0.14	0.94
	Tp (s)	10.90	0.24	1.88	0.02	0.17	0.72
	Dirp (deg)	266.50	-3.35	24.14	-0.01	0.09	0.73
Moray Forth	Hm0 (m)	1.26	-0.38	0.51	-0.30	0.41	0.91
	Tp (s)	7.59	2.55	5.82	0.34	0.77	0.23
	Dirp (deg)	141.91	-45.58	95.19	-0.32	0.67	0.42
Firth of Forth	Hm0 (m)	1.16	-0.15	0.26	-0.13	0.22	0.97
	Tp (s)	7.12	0.80	3.18	0.11	0.45	0.52
	Dirp (deg)	128.72	-13.06	75.44	-0.10	0.59	0.55

Table 4. Quality Indices-Jan 2012

Site	Wave parameters	Mean	Bias	RMSE	Bias/Mean	SI	R
Cefas	Hm0 (m)	4.90	0.45	0.75	0.09	0.15	0.96
	Tp (s)	12.89	0.28	1.37	0.02	0.11	0.81
	Dirp (deg)	271.66	-8.50	25.73	-0.03	0.09	0.53
Blackstone	Hm0 (m)	4.48	0.06	0.54	0.01	0.12	0.96
	Tp (s)	12.94	0.16	1.36	0.01	0.1	0.77
	Dirp (deg)	277.59	-11.88	24.45	-0.04	0.09	0.47
Moray Forth	Hm0 (m)	1.31	-0.37	0.55	-0.28	0.42	0.67
	Tp (s)	7.49	2.24	5.68	0.30	0.76	0.16
	Dirp (deg)	160.13	-70.40	117.84	-0.44	0.74	0.32
Firth of Forth	Hm0 (m)	1.07	-0.17	0.31	-0.16	0.29	0.86
	Tp (s)	6.50	1.27	3.42	0.20	0.53	0.35
	Dirp (deg)	156.37	61.88	113.81	0.40	0.73	0.27

Table 5. Quality Indices-March 2012

Site	Wave parameters	Mean	Bias	RMSE	Bias/Mean	SI	R
Cefas	Hm0 (m)	3.79	0.36	0.59	0.10	0.16	0.97
	Tp (s)	12.85	0.17	1.42	0.01	0.11	0.82
	Dirp (deg)	269.44	-8.32	19.67	-0.03	0.07	0.71
Blackstone	Hm0 (m)	3.25	0.02	0.47	0.01	0.14	0.95
	Tp (s)	12.75	0.18	1.53	0.01	0.12	0.78
	Dirp (deg)	280.41	-16.62	22.74	-0.06	0.08	0.52
Moray Forth	Hm0 (m)	0.87	-0.38	0.47	-0.44	0.54	0.80
	Tp (s)	8.58	2.45	5.84	0.29	0.68	0.33
	Dirp (deg)	136.92	-56.45	111.21	-0.41	0.81	0.21
Firth of Forth	Hm0 (m)	0.62	-0.16	0.23	-0.25	0.37	0.88
	Tp (s)	6.58	1.66	5.21	0.25	0.79	0.08
	Dirp (deg)	128.08	-27.09	102.51	-0.21	0.80	0.31

Table 6. Quality indices for Jan-Dec 2010

Site	Wave parameters	Mean	Bias	RMSE	Bias/Mean	SI	R
Cefas	Hm0 (m)	2.28	0.27	0.44	0.12	0.19	0.95
	Tp (s)	10.44	0.42	1.71	0.04	0.16	0.72
	Dirp (deg)	283.5	-16.94	40.93	-0.06	0.14	0.59
Blackstone	Hm0 (m)	2.03	0.23	0.45	0.11	0.22	0.94
	Tp (s)	10.15	0.61	2.02	0.06	0.20	0.71
	Dirp(deg)	268.09	-6.85	48.44	-0.03	0.18	0.61
Moray Forth	Hm0 (m)	1.13	-0.16	0.34	-0.14	0.30	0.94
	Tp (s)	7.58	0.11	3.01	0.01	0.40	0.39
	Dirp(deg)	100.96	-36.90	84.78	-0.37	0.84	0.27
Firth of Forth	Hm0 (m)	1.15	-0.10	0.25	-0.09	0.22	0.96
	Tp (s)	7.40	-0.13	1.85	-0.02	0.25	0.64
	Dirp(deg)	86.50	-17.14	55.97	-0.20	0.65	0.57
Orkney	Hm0 (m)	1.67	0.03	0.31	0.02	0.19	0.95
	Tp (s)	10.21	0.45	1.96	0.04	0.19	0.69
	Dirp(deg)	304.41	-6.13	22.23	-0.02	0.07	0.75

Figures

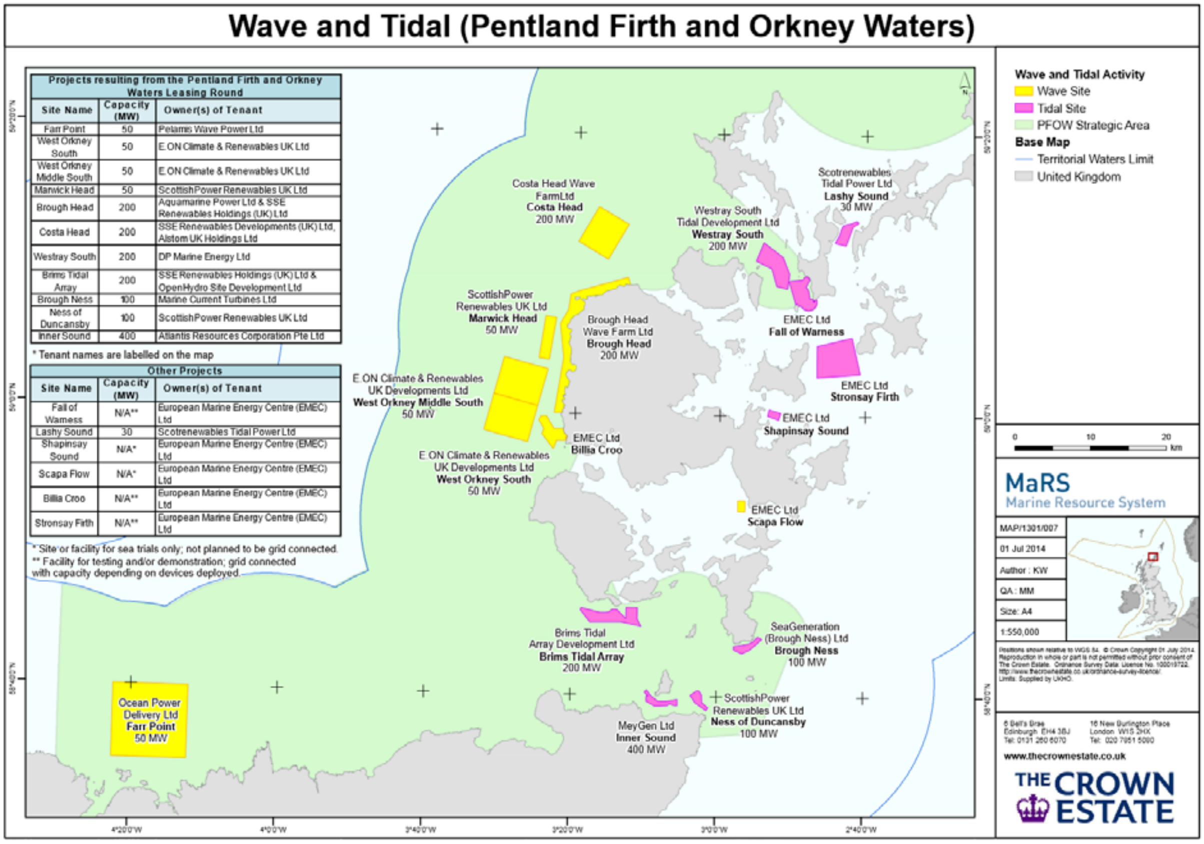

Figure 1. Location of Pentland Firth showing wave and tidal energy leasing sites [2].

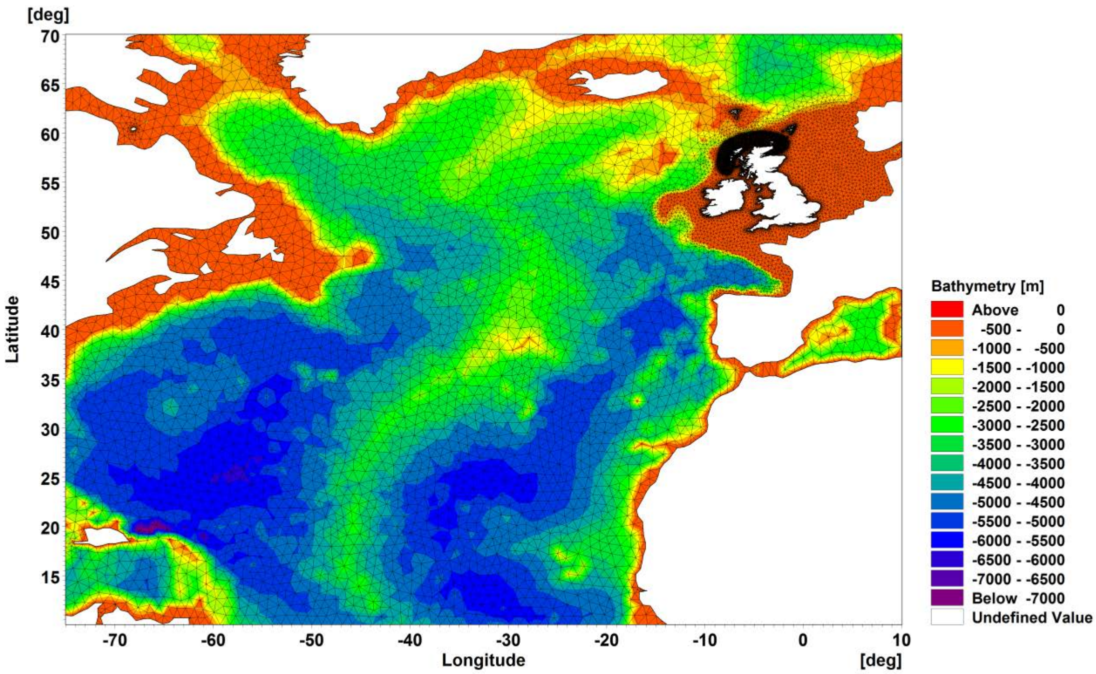

Figure 2. Computational domain for North Atlantic wave model

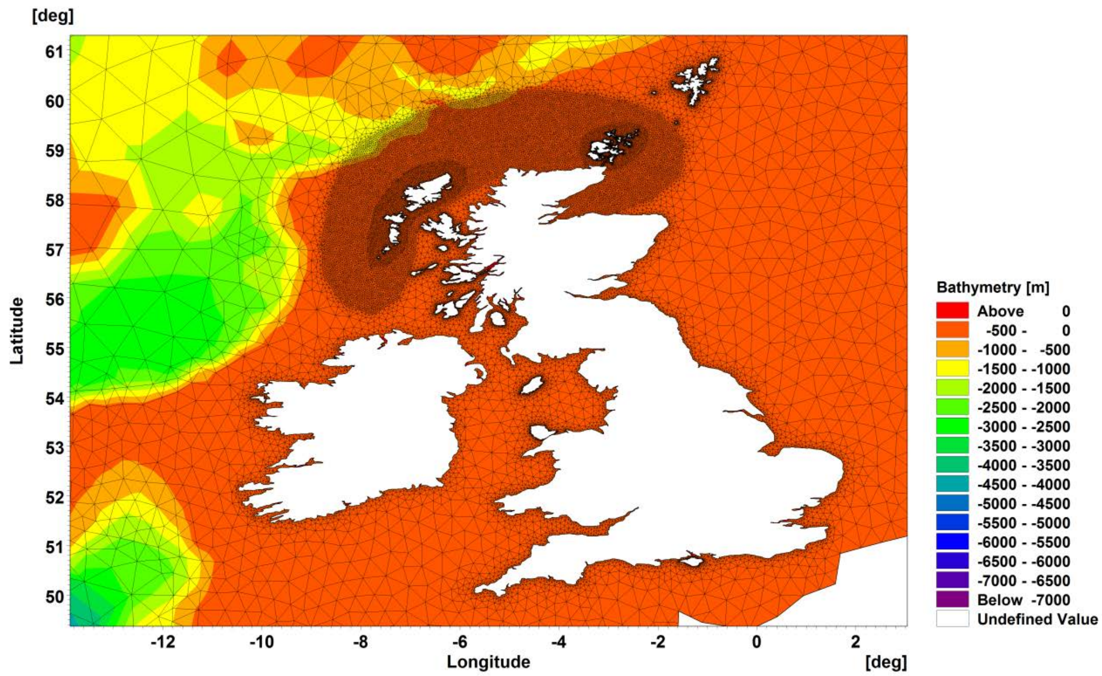

Figure 3. Enlarged view of the computational mesh for UK/Scotland

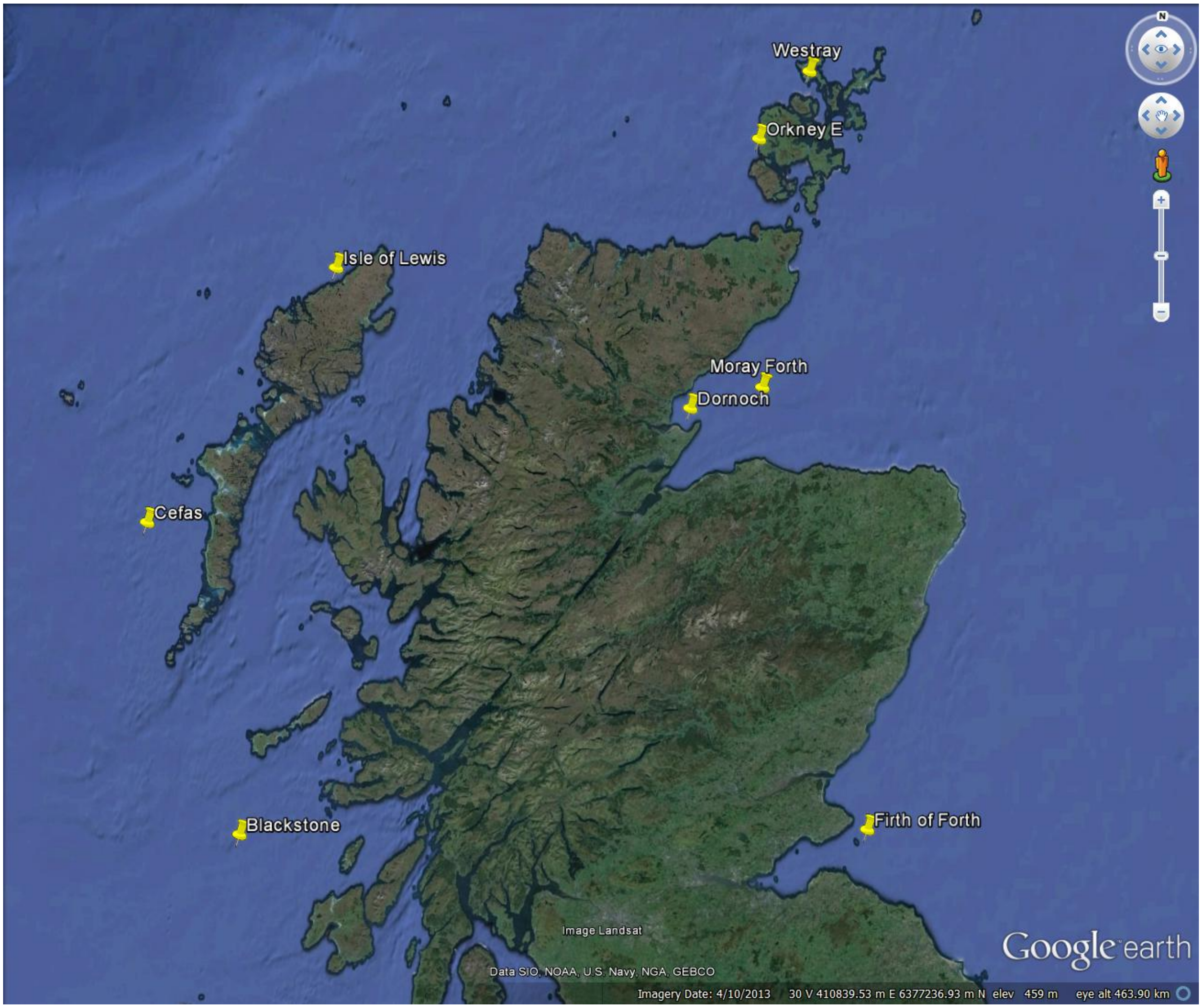

Figure 4. Location of wave buoys in google earth.

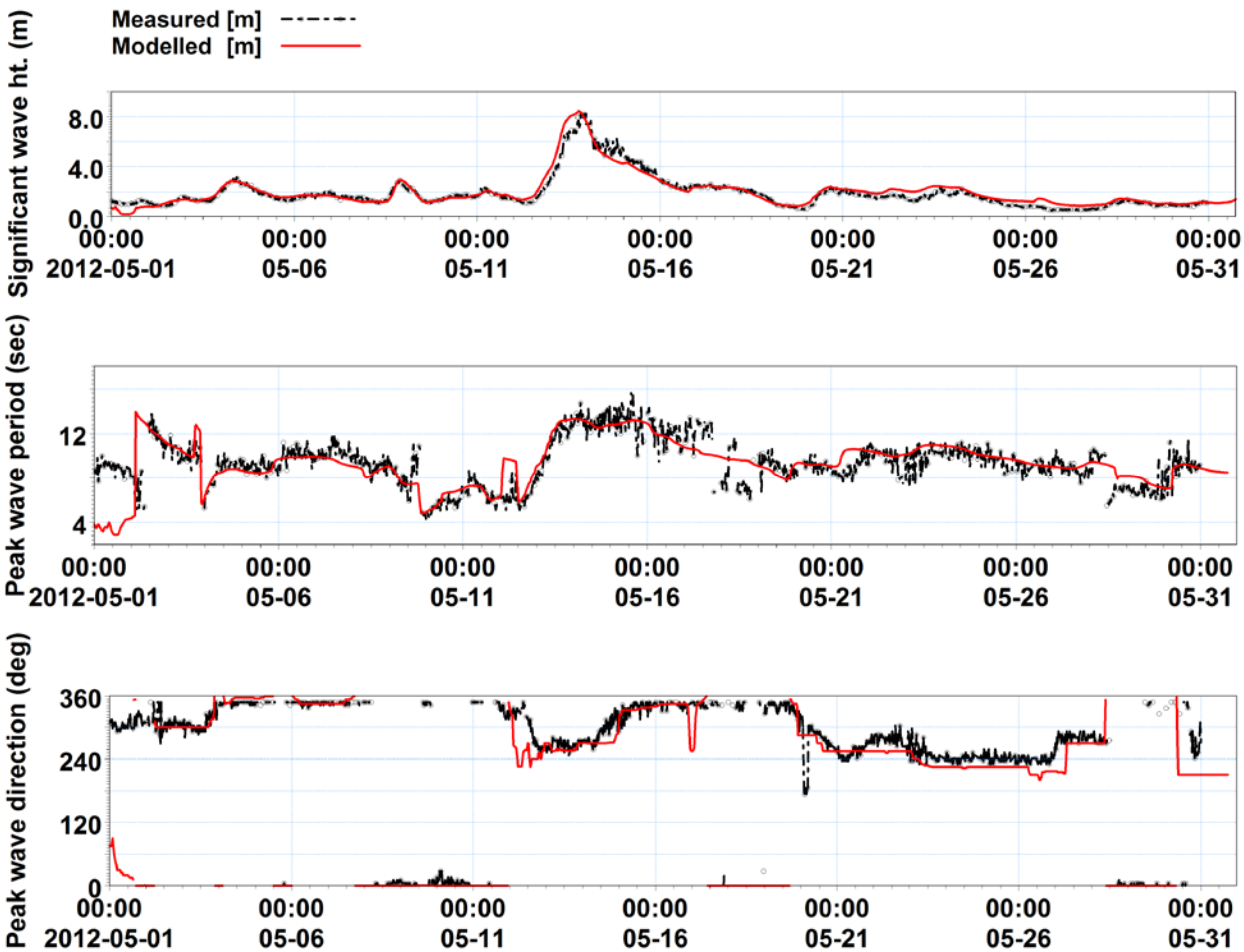

Figure 5. Comparison of significant wave height, peak wave period and peak wave direction between model and Cefas wave buoy, for May 2012; Model calibration phase.

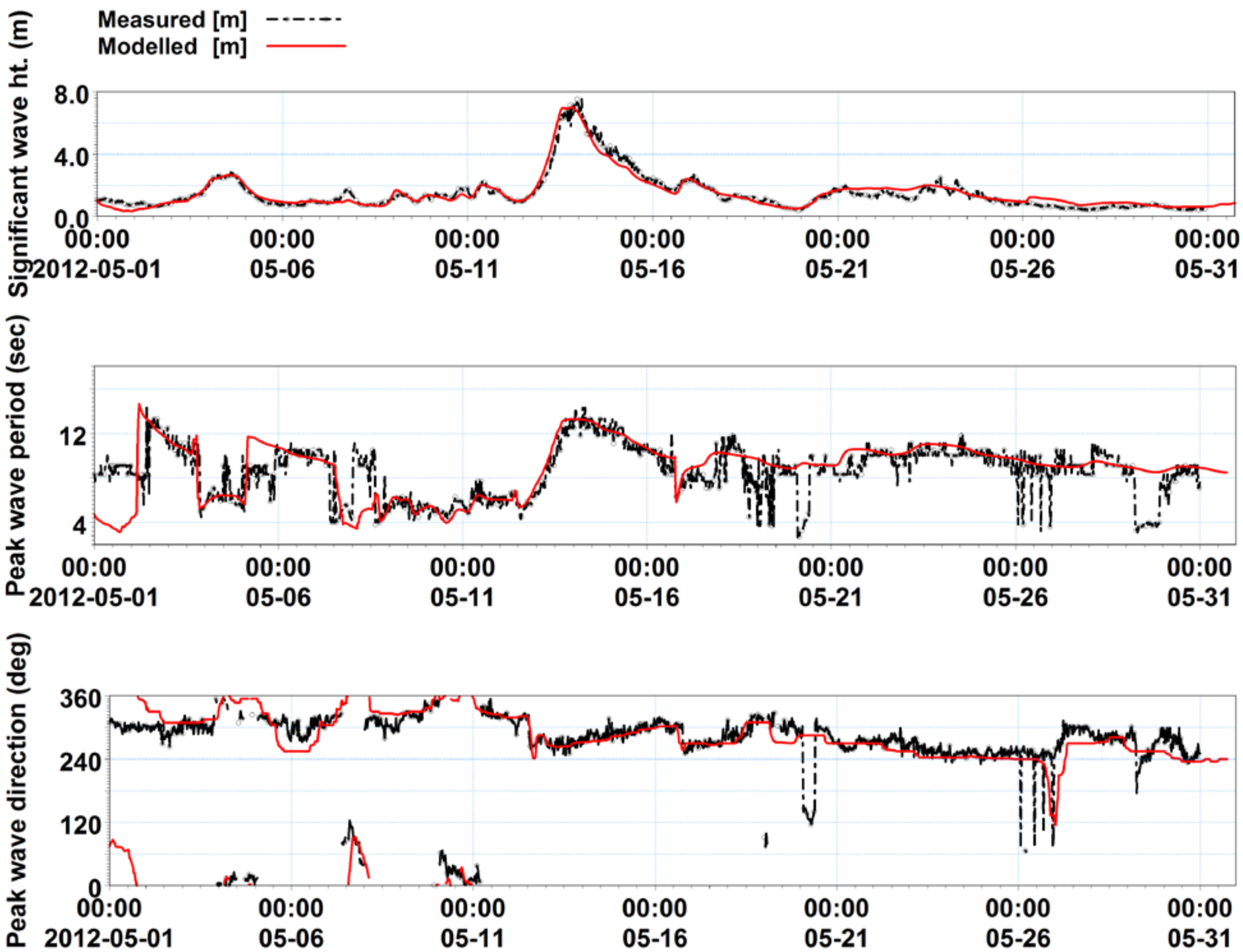

Figure 6. Comparison of significant wave height, peak wave period and peak wave direction between model and Blackstone wave buoy, for May 2012; Model calibration phase.

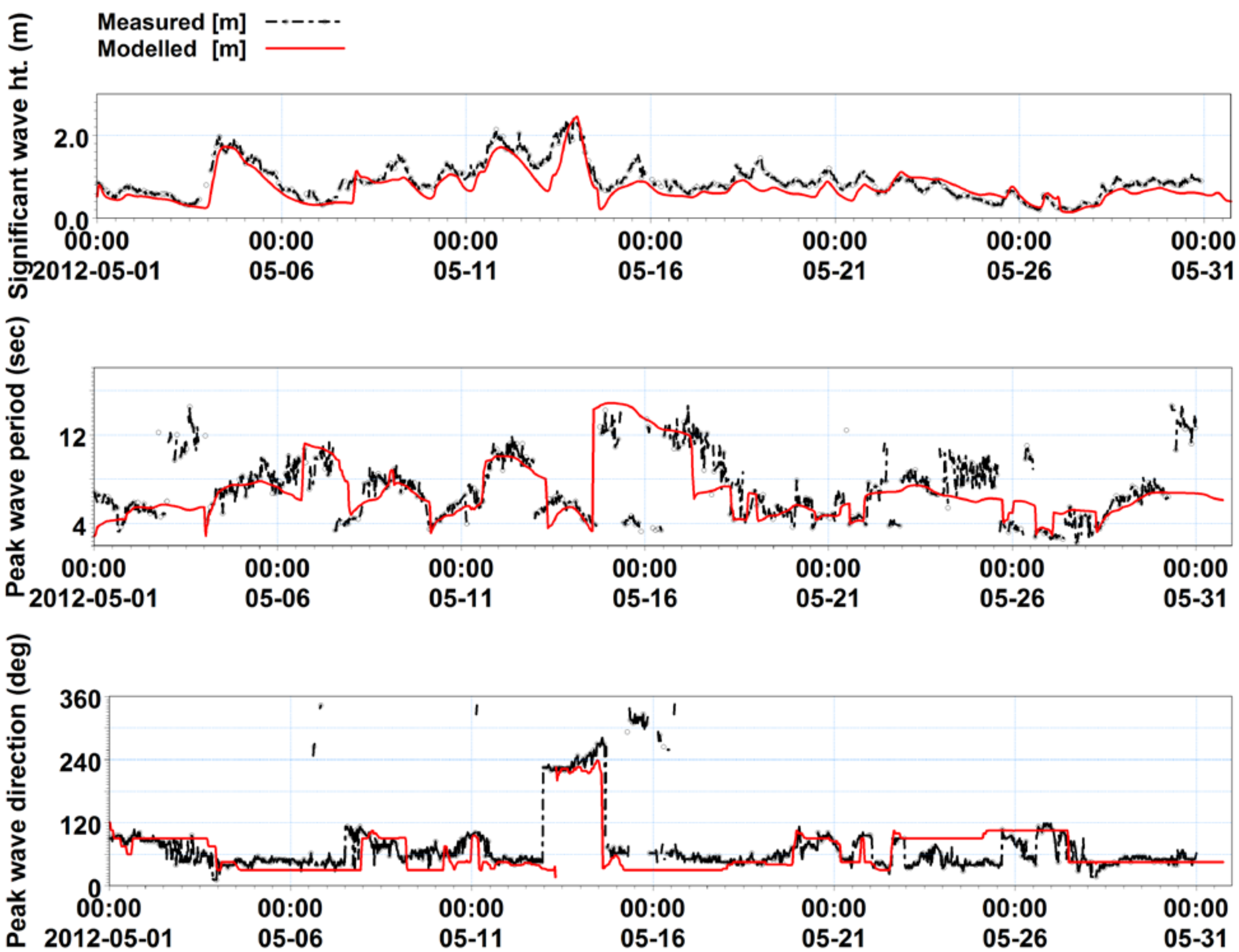

Figure 7. Comparison of significant wave height, peak wave period and peak wave direction between model and Moray Firth wave buoy, for May 2012; Model calibration phase.

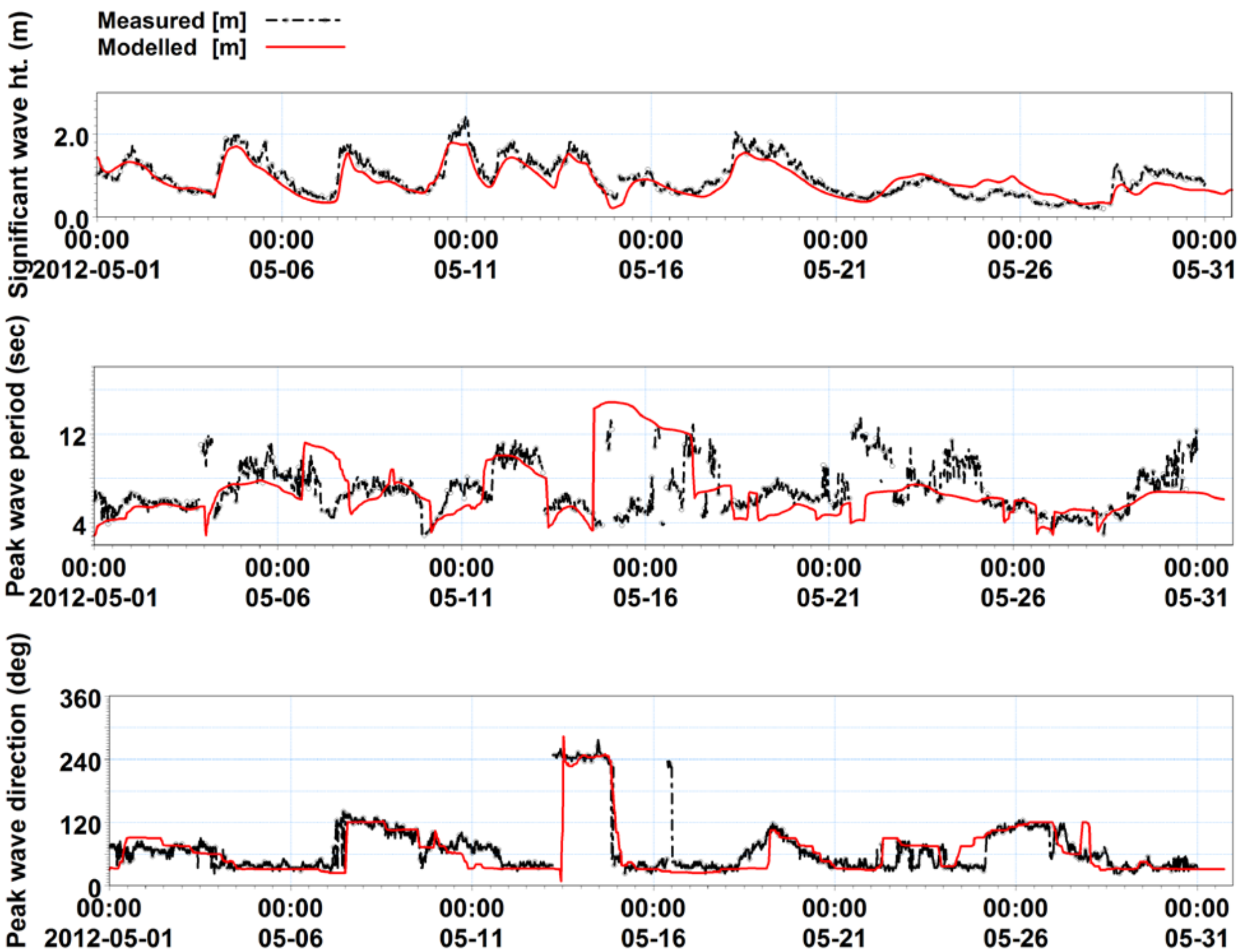

Figure 8. Comparison of significant wave height, peak wave period and peak wave direction between model and Firth of Forth wave buoy, for May 2012; Model calibration phase.

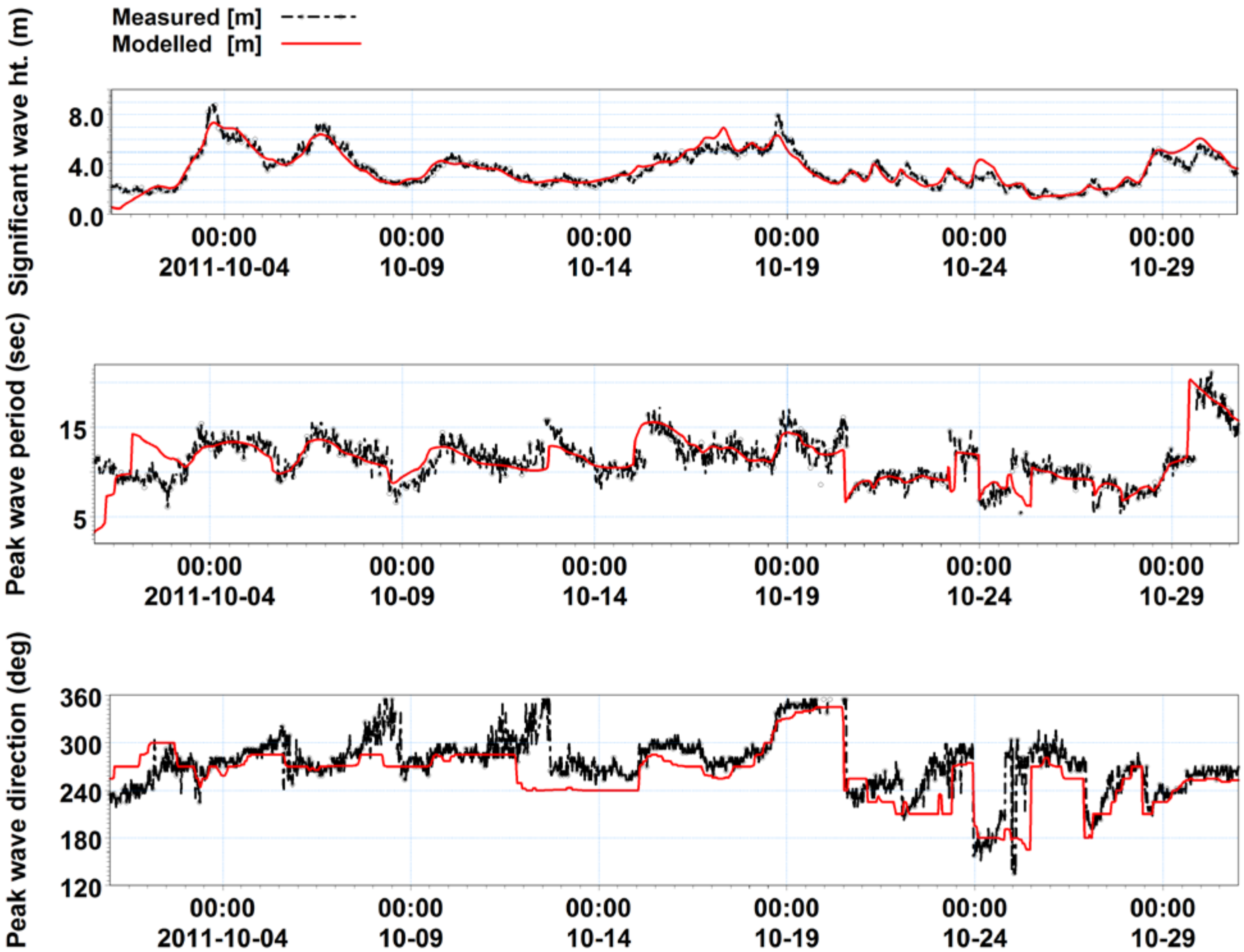

Figure 9. Comparison of significant wave height, peak wave period and peak wave direction between model and Cefas wave buoy, for October 2011; Model validation phase.

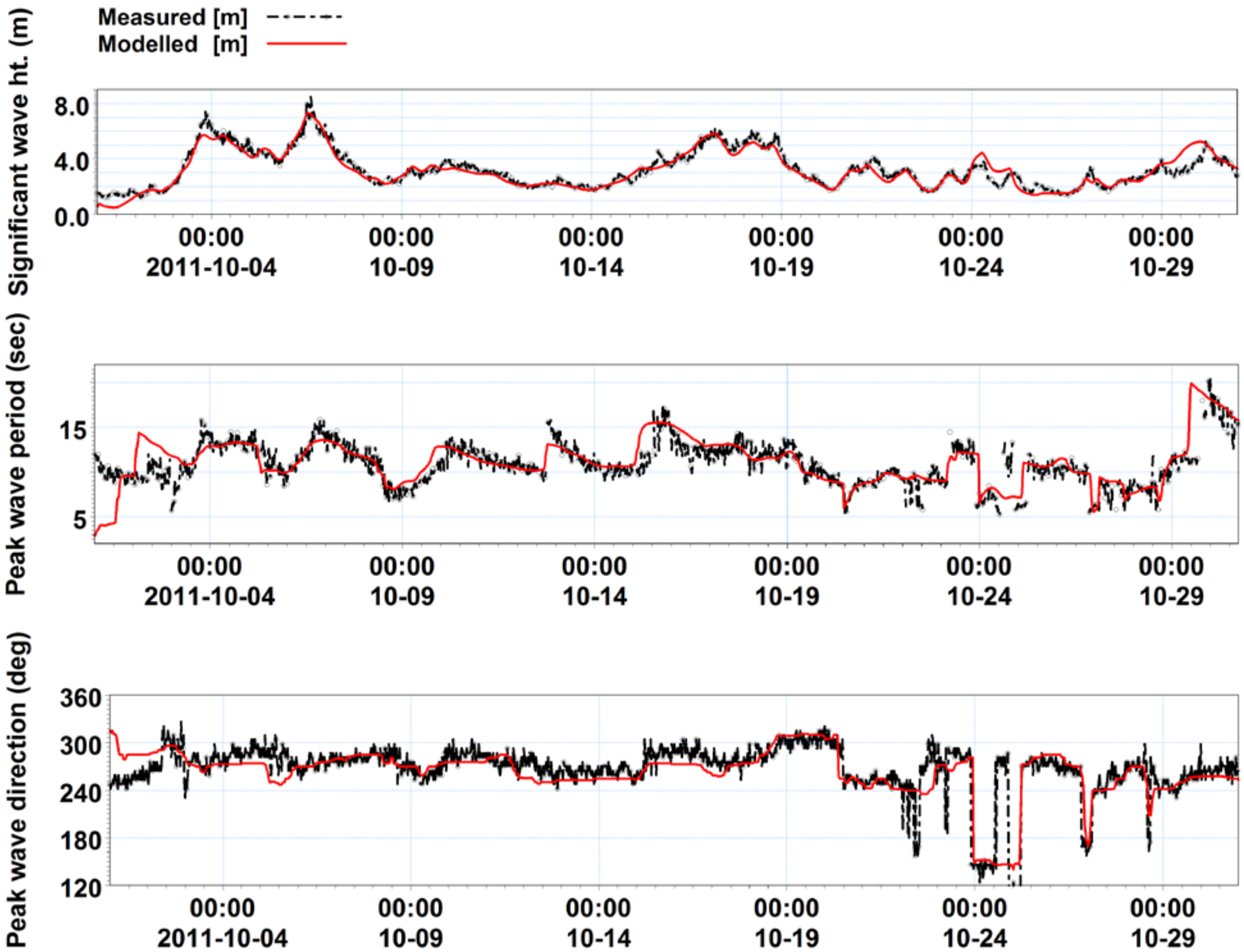

Figure 10. Comparison of significant wave height, peak wave period and peak wave direction between model and Blackstone wave buoy, for October 2011; Model validation phase.

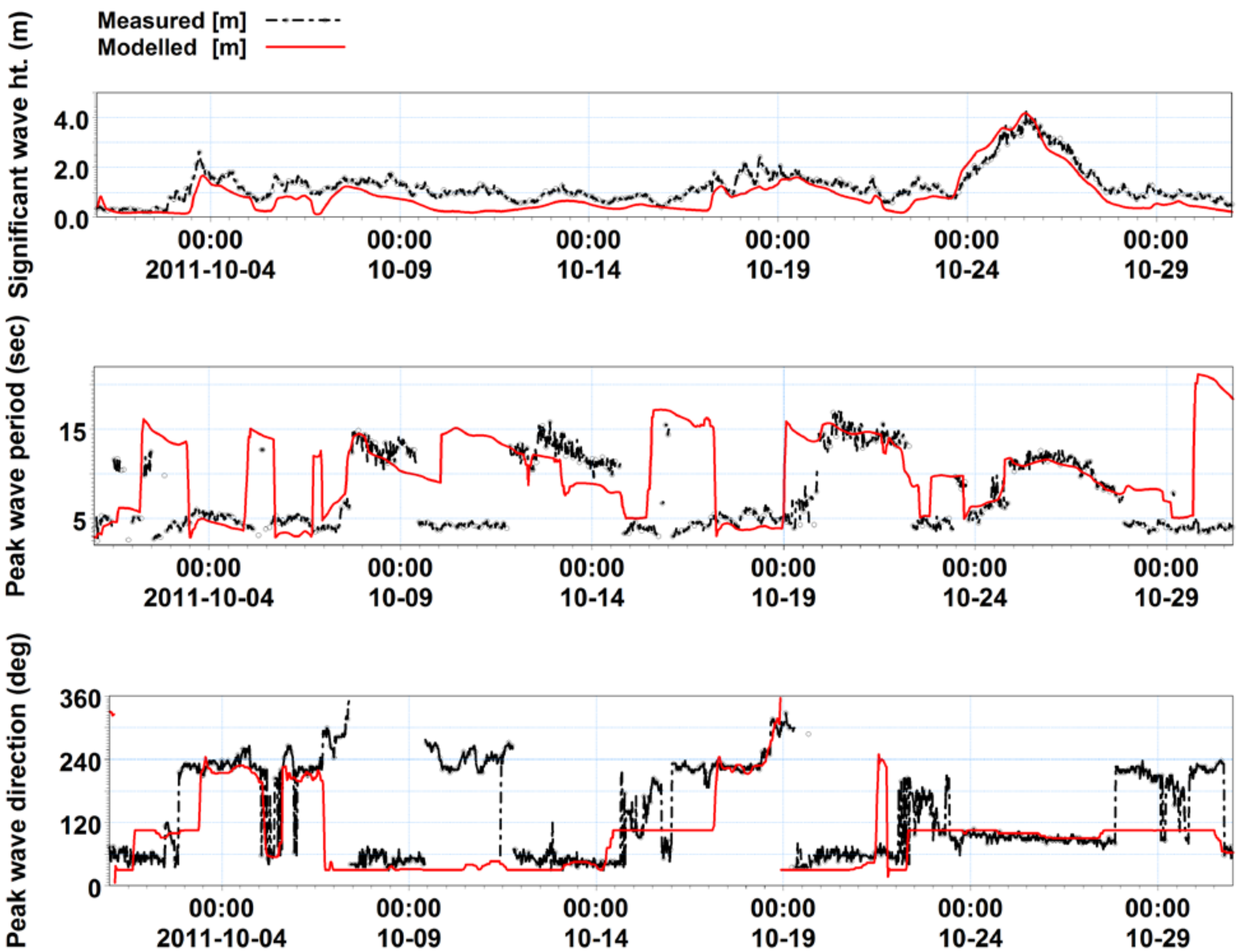

Figure 11. Comparison of significant wave height, peak wave period and peak wave direction between model and Moray Firth wave buoy, for October 2011; Model validation phase.

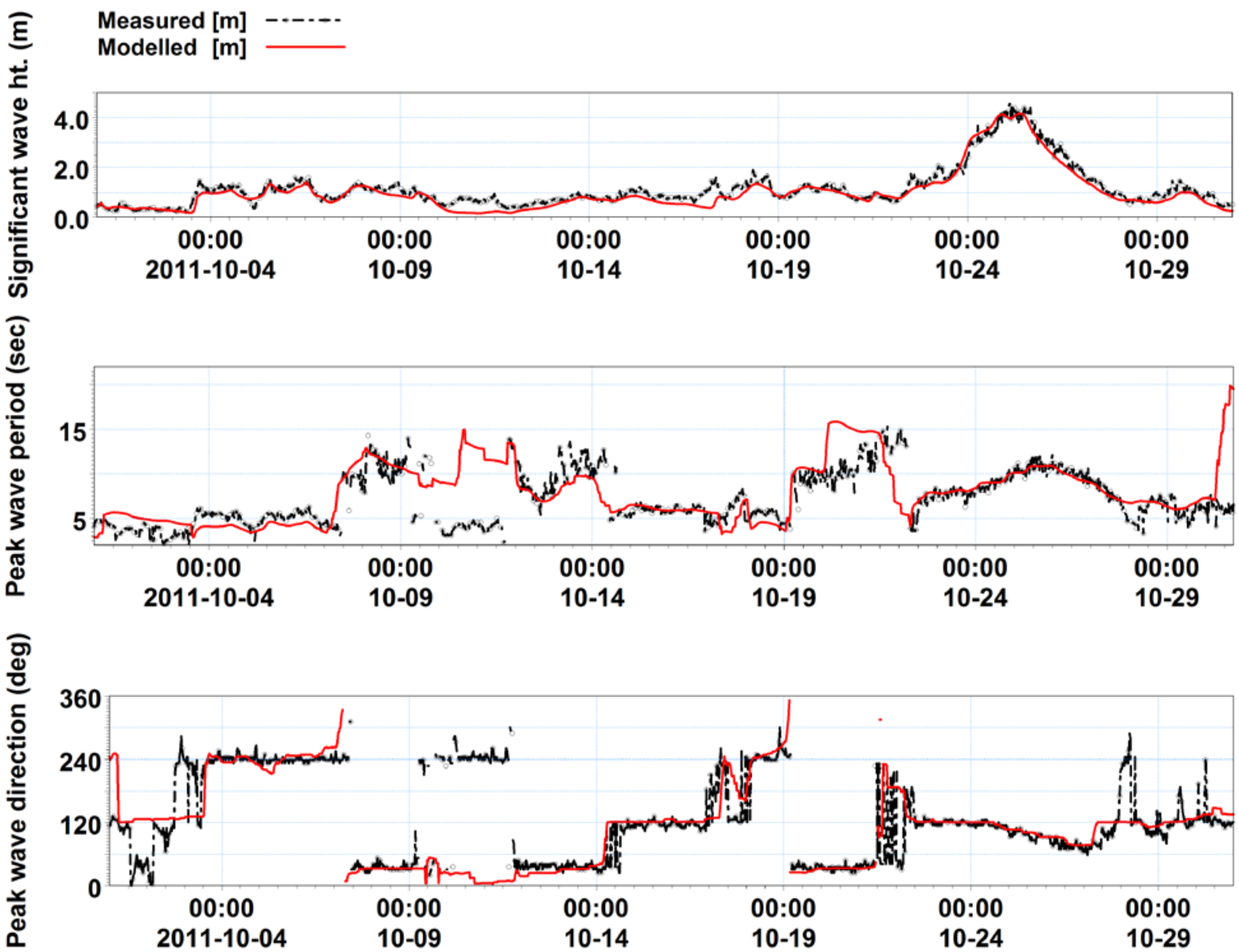

Figure 12. Comparison of significant wave height, peak wave period and peak wave direction between model and Firth of Forth wave buoy, for October 2011; Model validation phase.

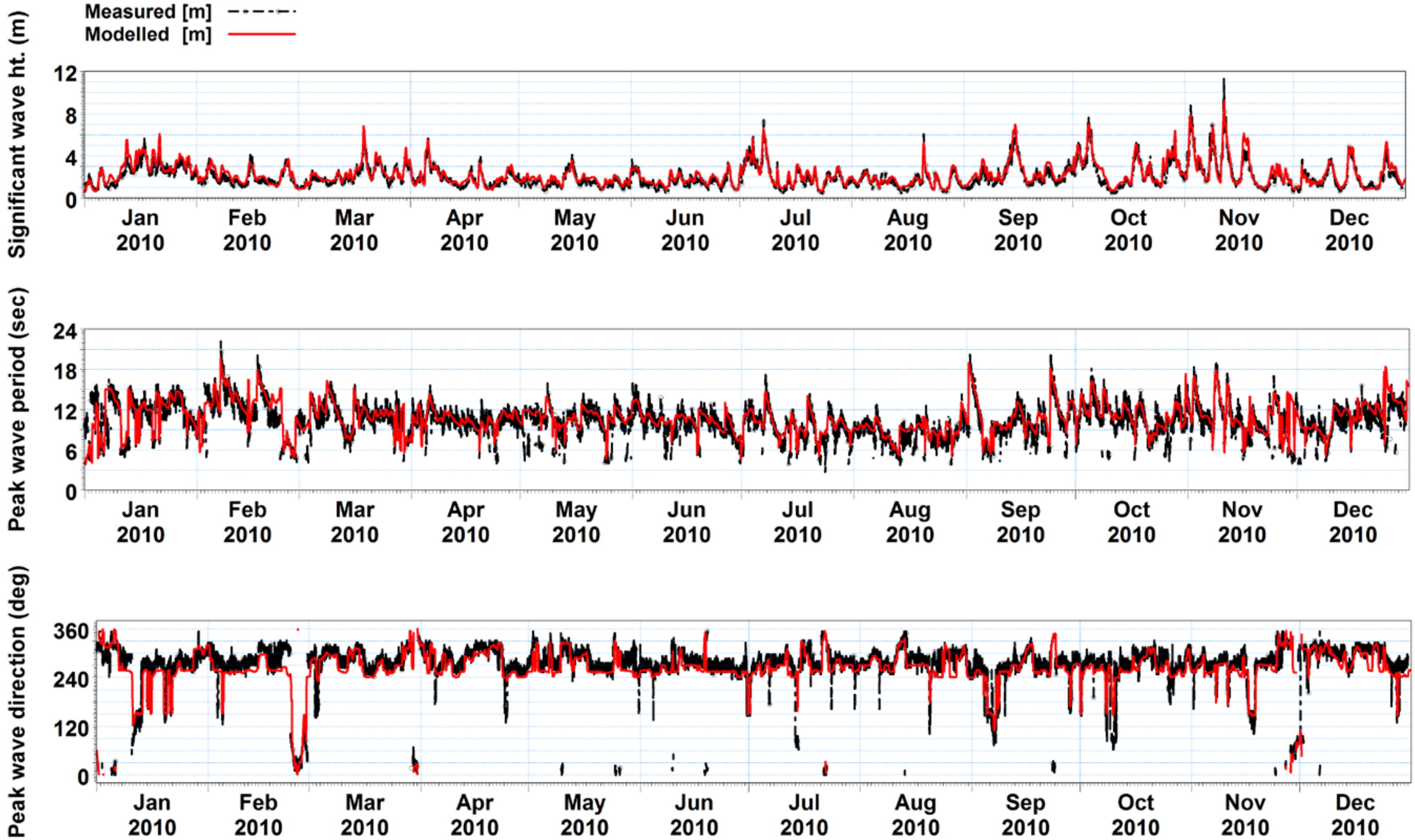

Figure 13. Comparison of significant wave height, peak wave period and peak wave direction between model and Blackstone wave buoy, for January-December 2010.

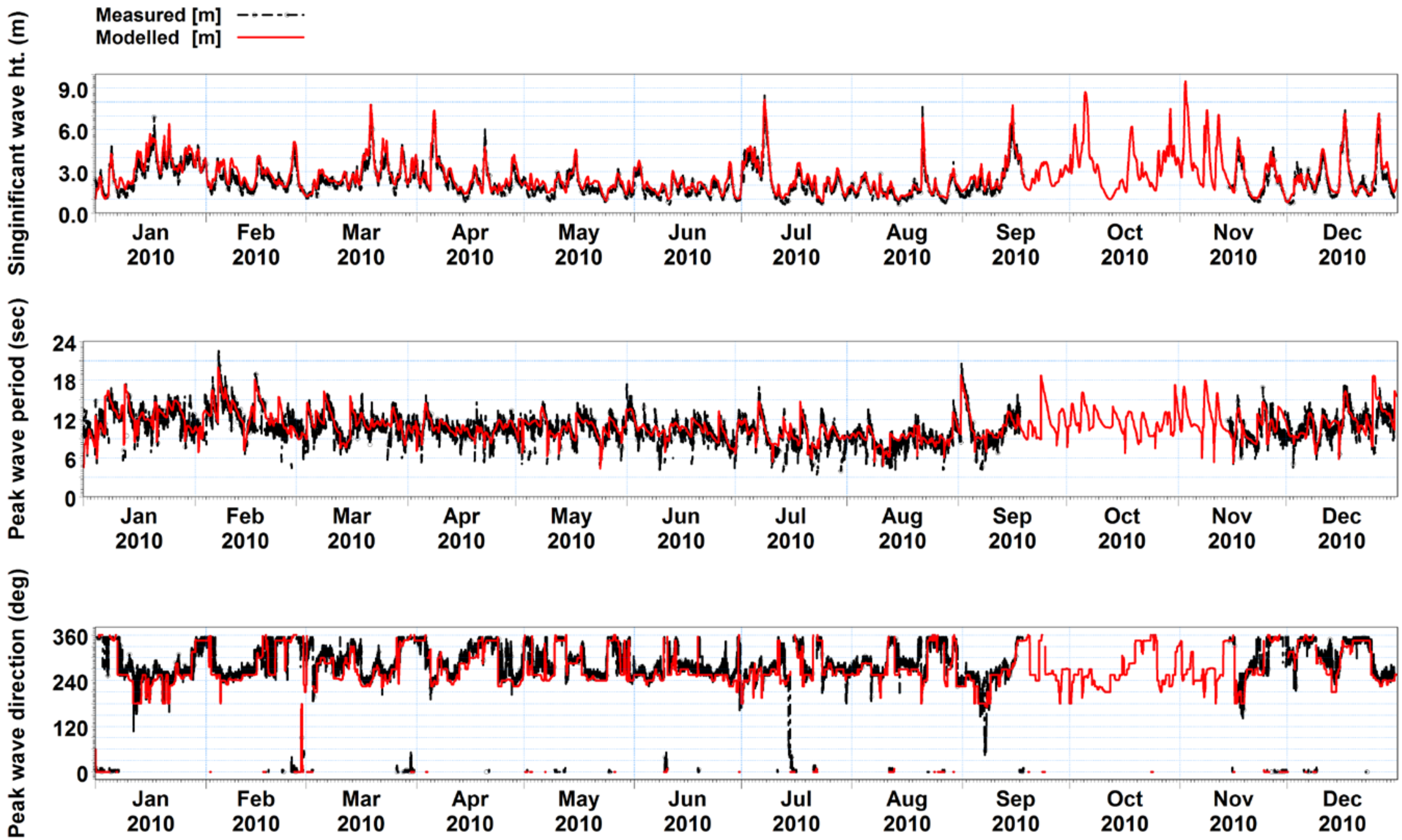

Figure 14. Comparison of significant wave height, peak wave period and peak wave direction between model and Cefas wave buoy, for January-December 2010.

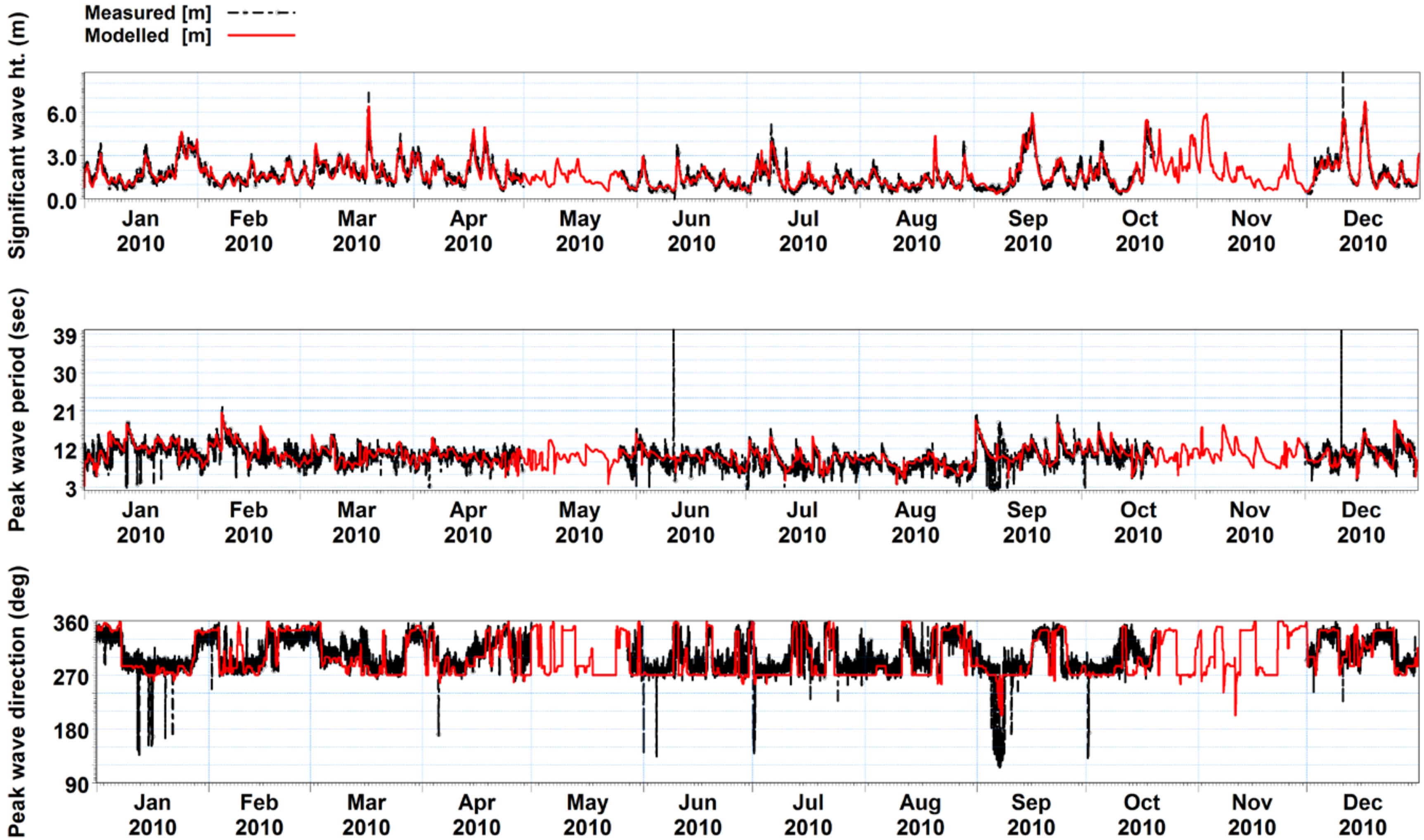

Figure 15. Comparison of significant wave height, peak wave period and peak wave direction between model and Orkney wave buoy, for January-December 2010.

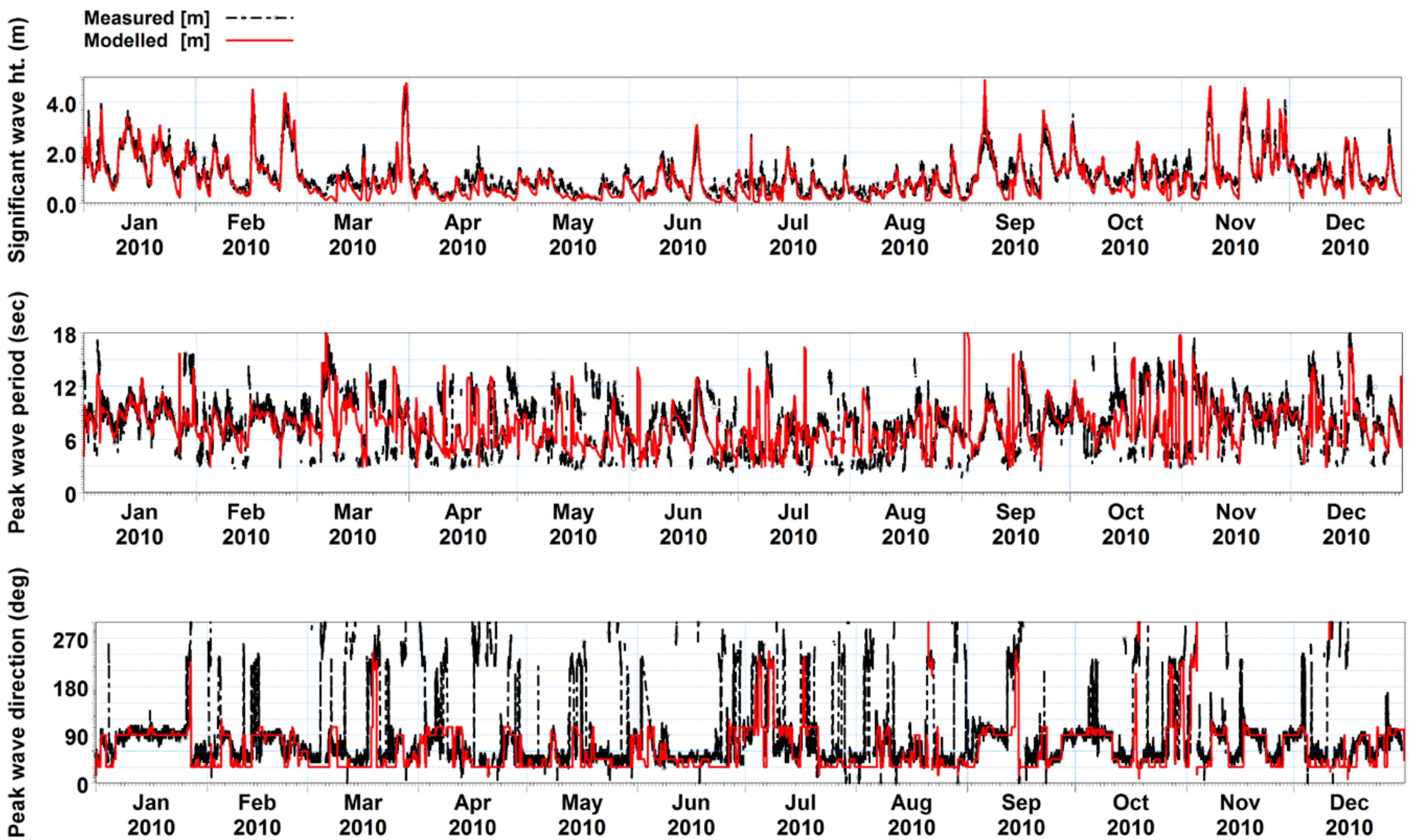

Figure 16. Comparison of significant wave height, peak wave period and peak wave direction between model and Moray Firth wave buoy, for January-December 2010.

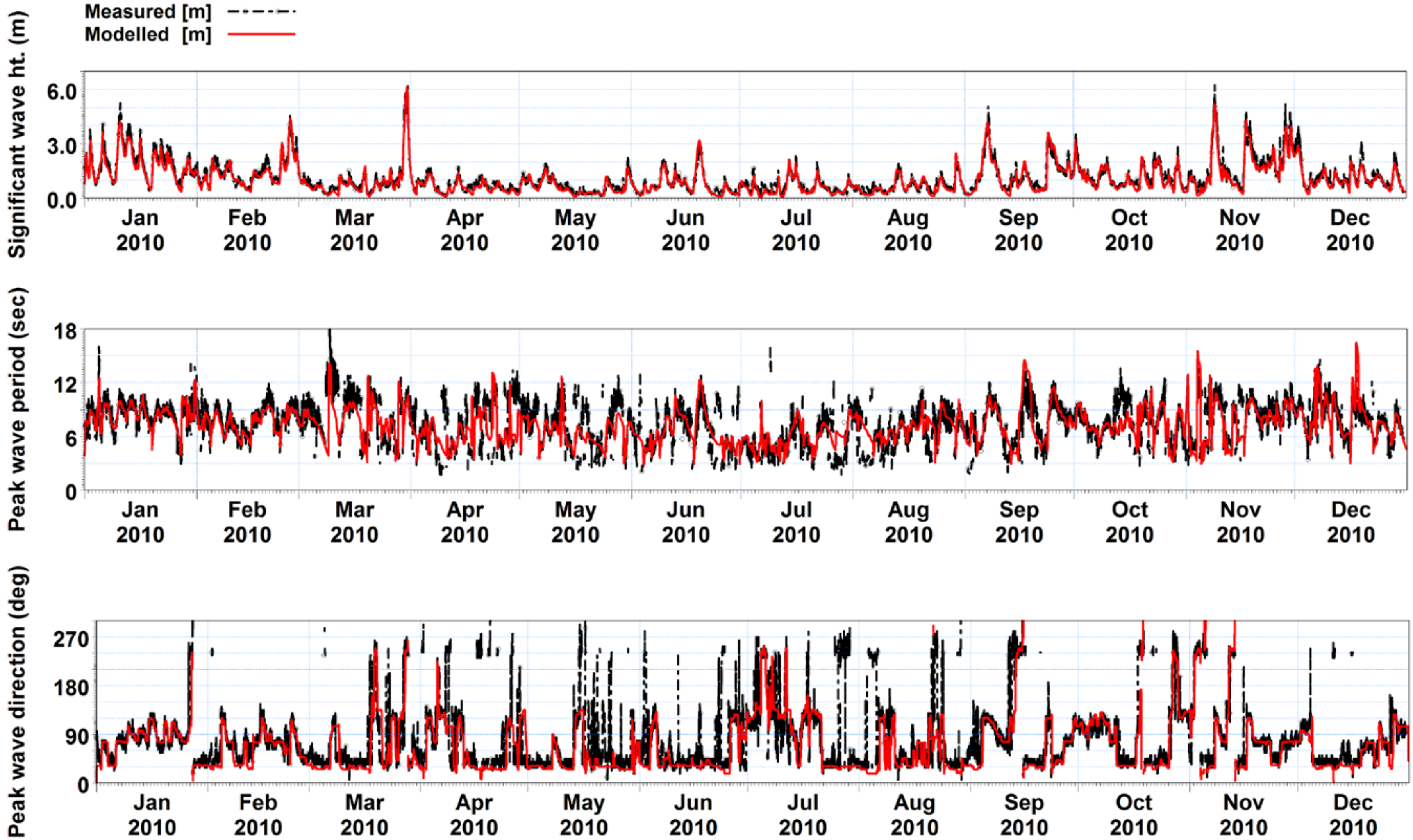

Figure 17. Comparison of significant wave height, peak wave period and peak wave direction between model and Firth of Forth wave buoy, for January-December 2010.

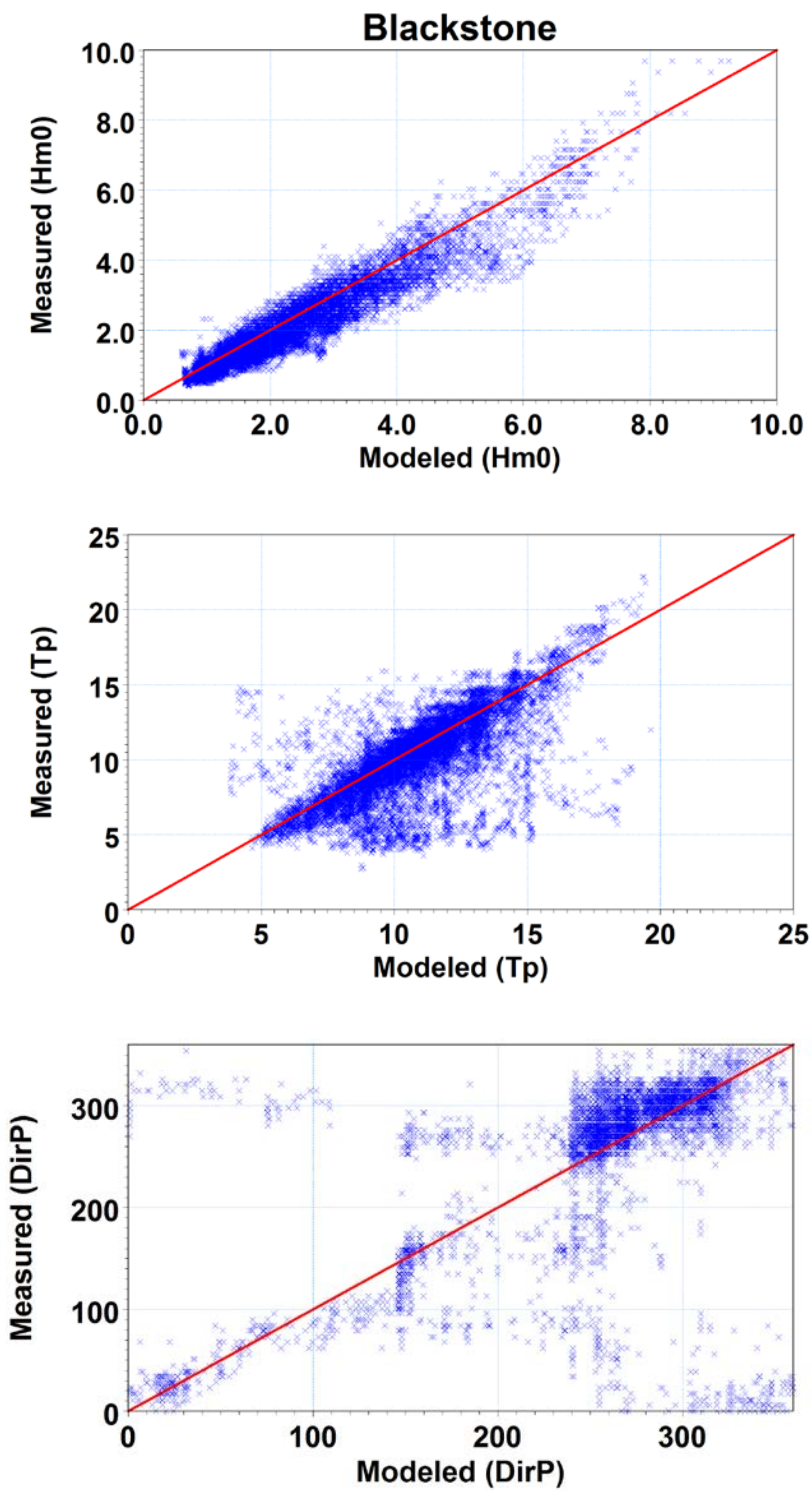

Figure 18. Correlation plots for significant wave height (H_{m0}), peak wave period (T_p) and peak wave direction (Dir_p) between model and measurements for Blackstone buoy, for January-December 2010.

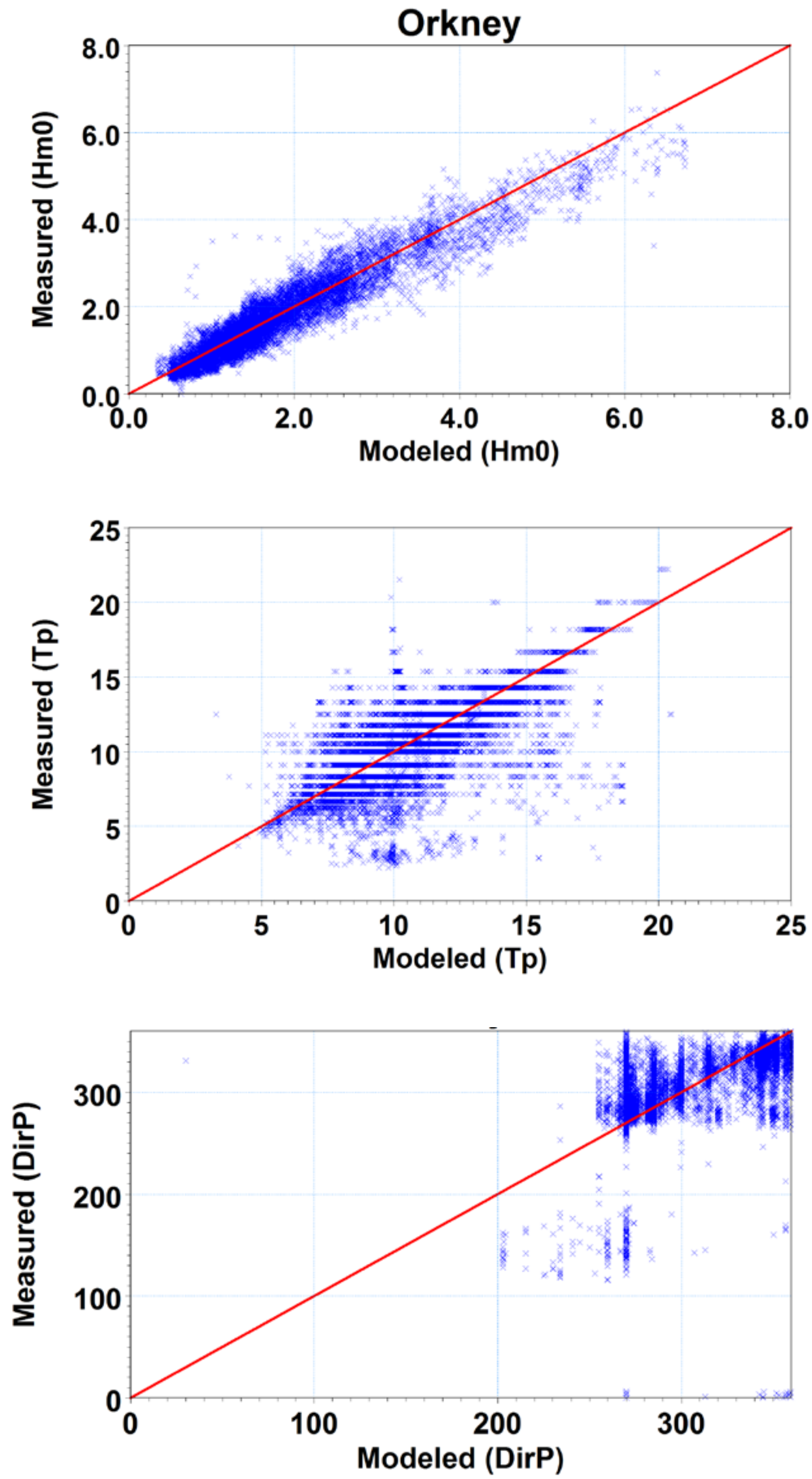

Figure 19. Correlation plots for significant wave height (H_{m0}), peak wave period (T_p) and peak wave direction (Dir_p) between model and measurements for Orkney buoy, for January-December 2010

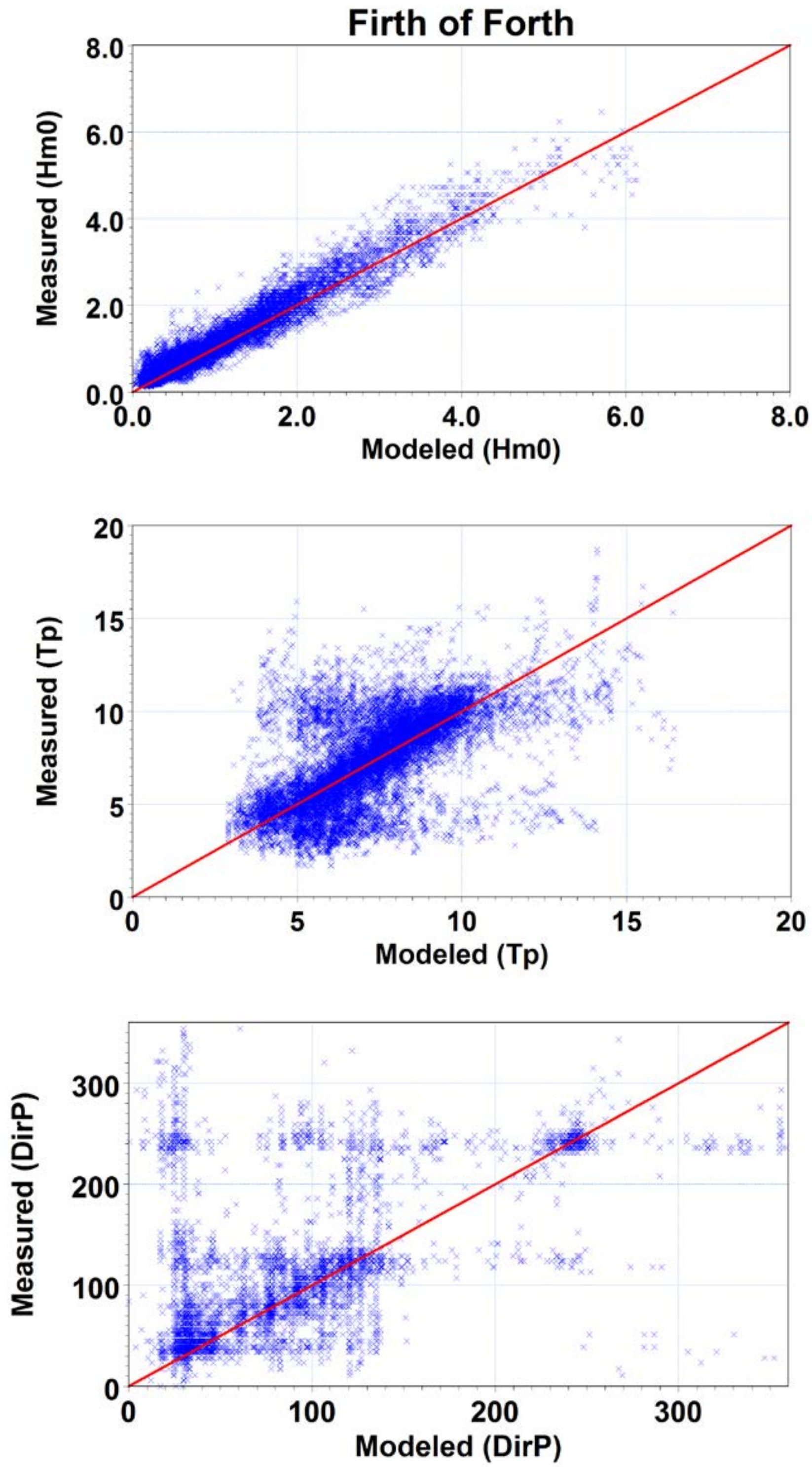

Figure 20. Correlation plots for significant wave height (H_{m0}), peak wave period (T_p) and peak wave direction (Dir_p) between model and measurements for Firth of Forth buoy, for January-December 2010

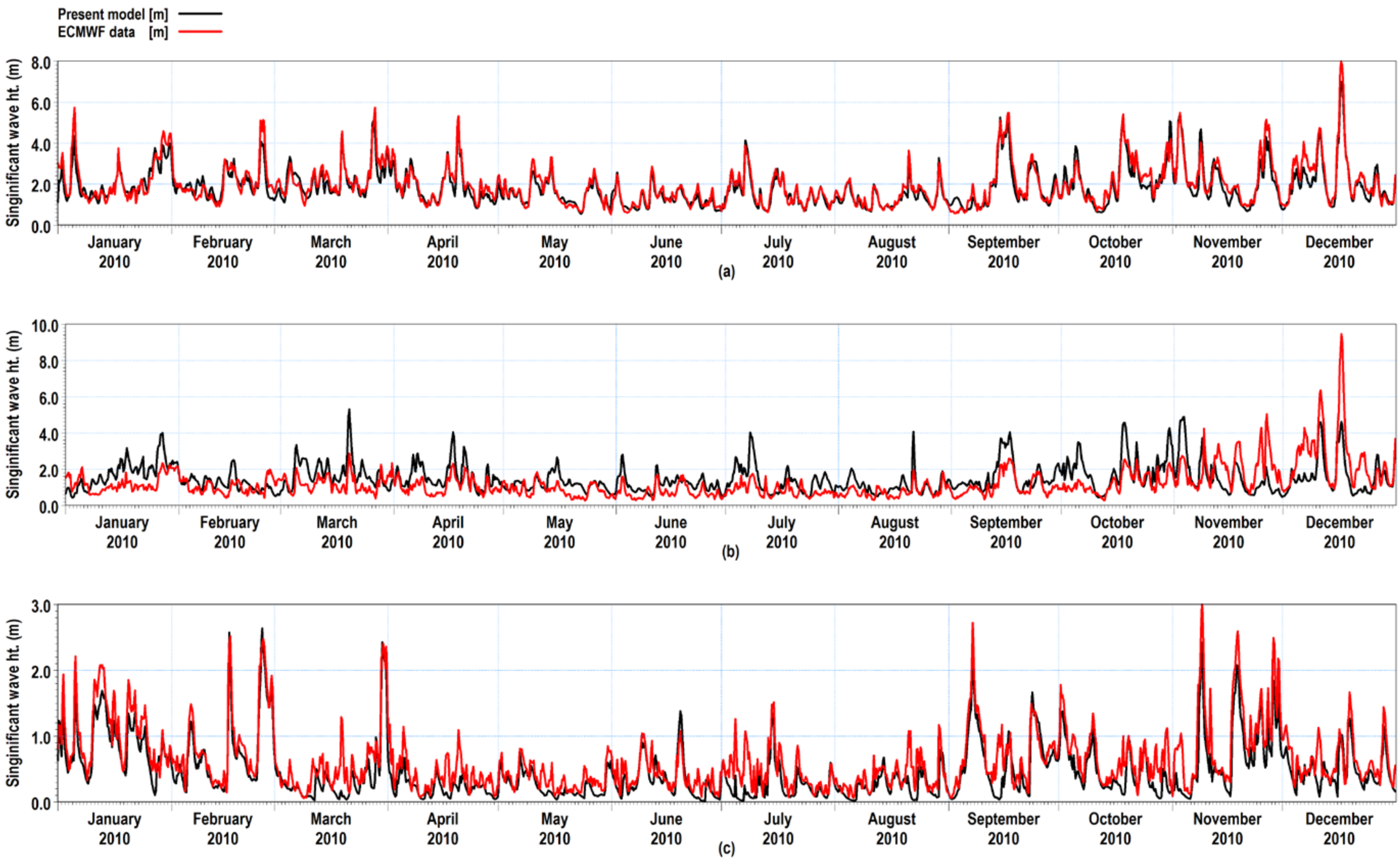

Figure 21. Comparison of significant wave height from MIKE21 and WAM models for shallow water locations: (a) Isle of Lewis, (b) Westray and (c) Dornoch for January-December 2010.

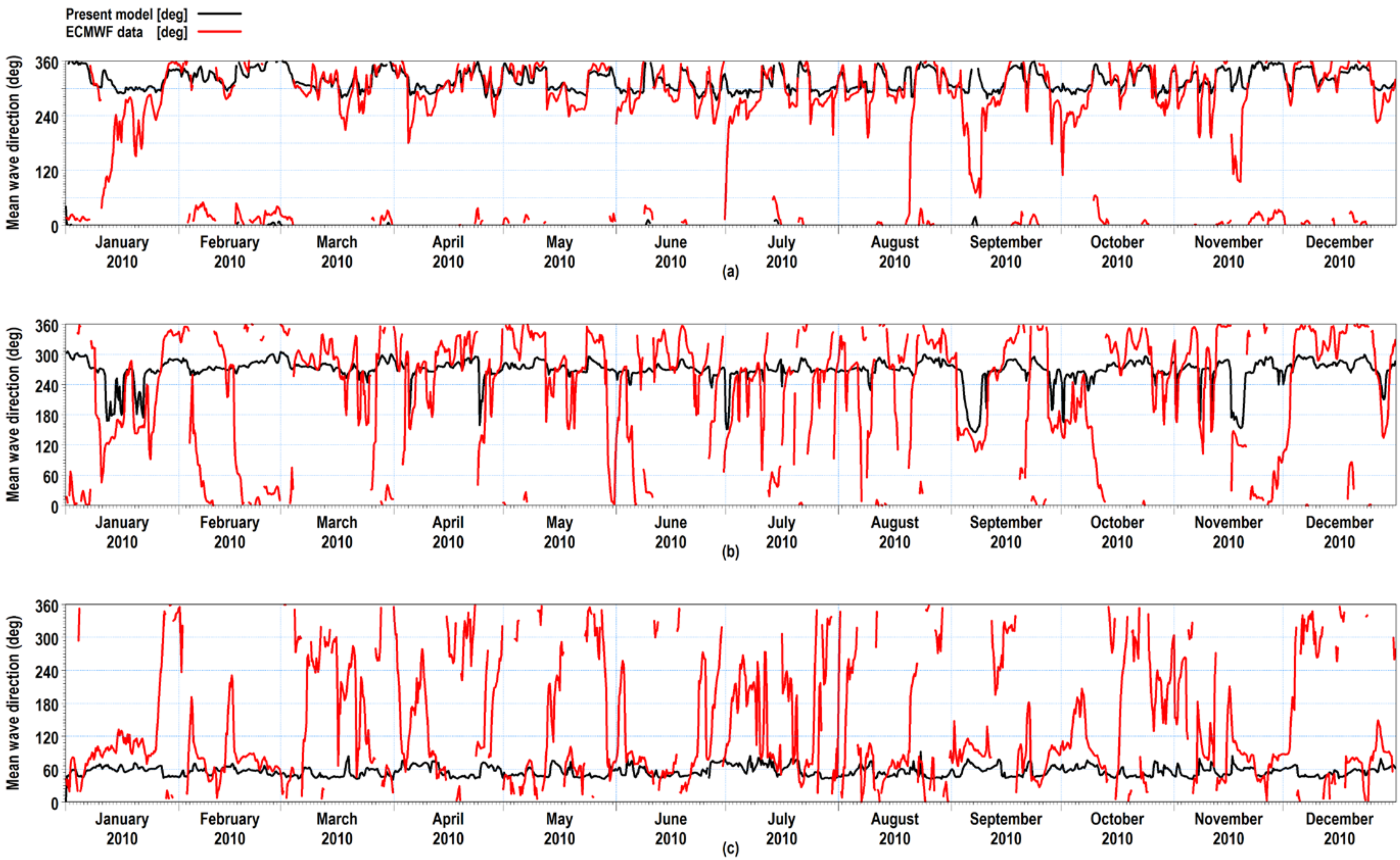

Figure 22. Comparison of mean wave direction from MIKE21 and WAM models for shallow water locations: (a) Isle of Lewis, (b) Westray and (c) Dornoch for January-December 2010.

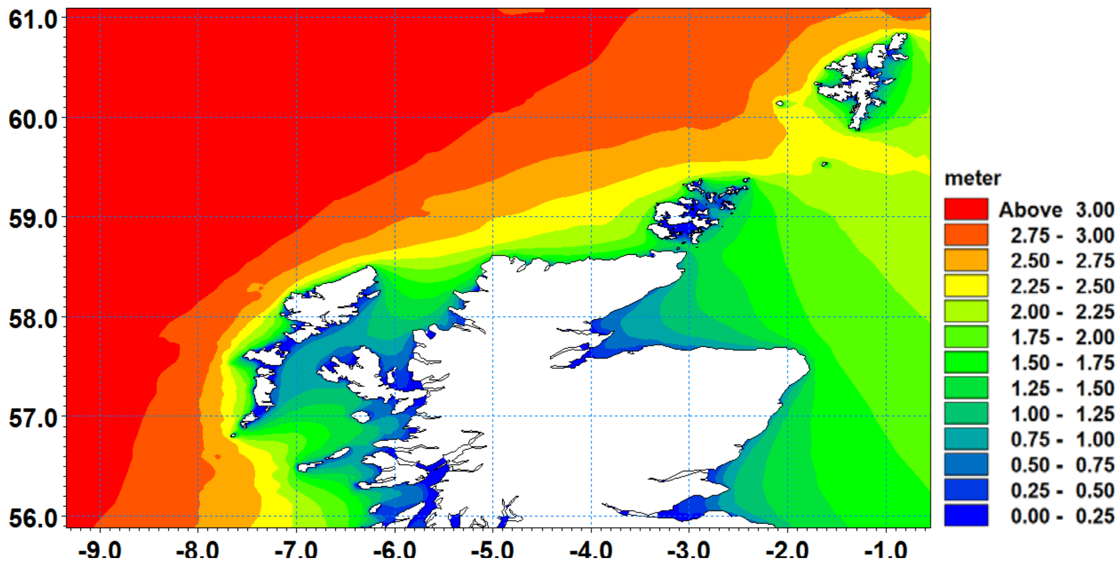

Figure 23. Mean significant wave height for January-December 2010

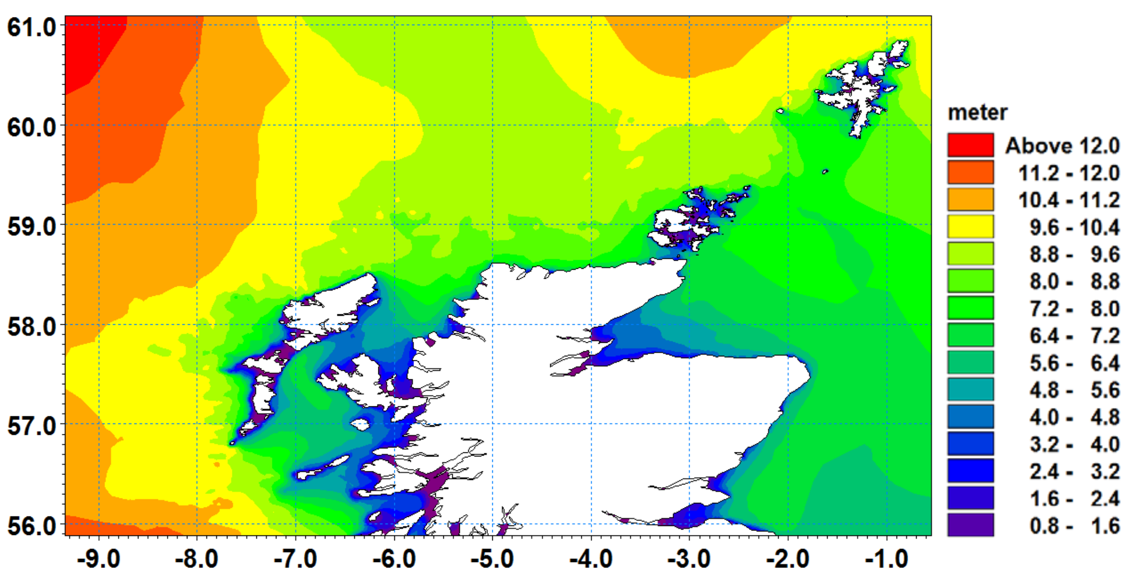

Figure 24. Maximum significant wave height for January-December 2010

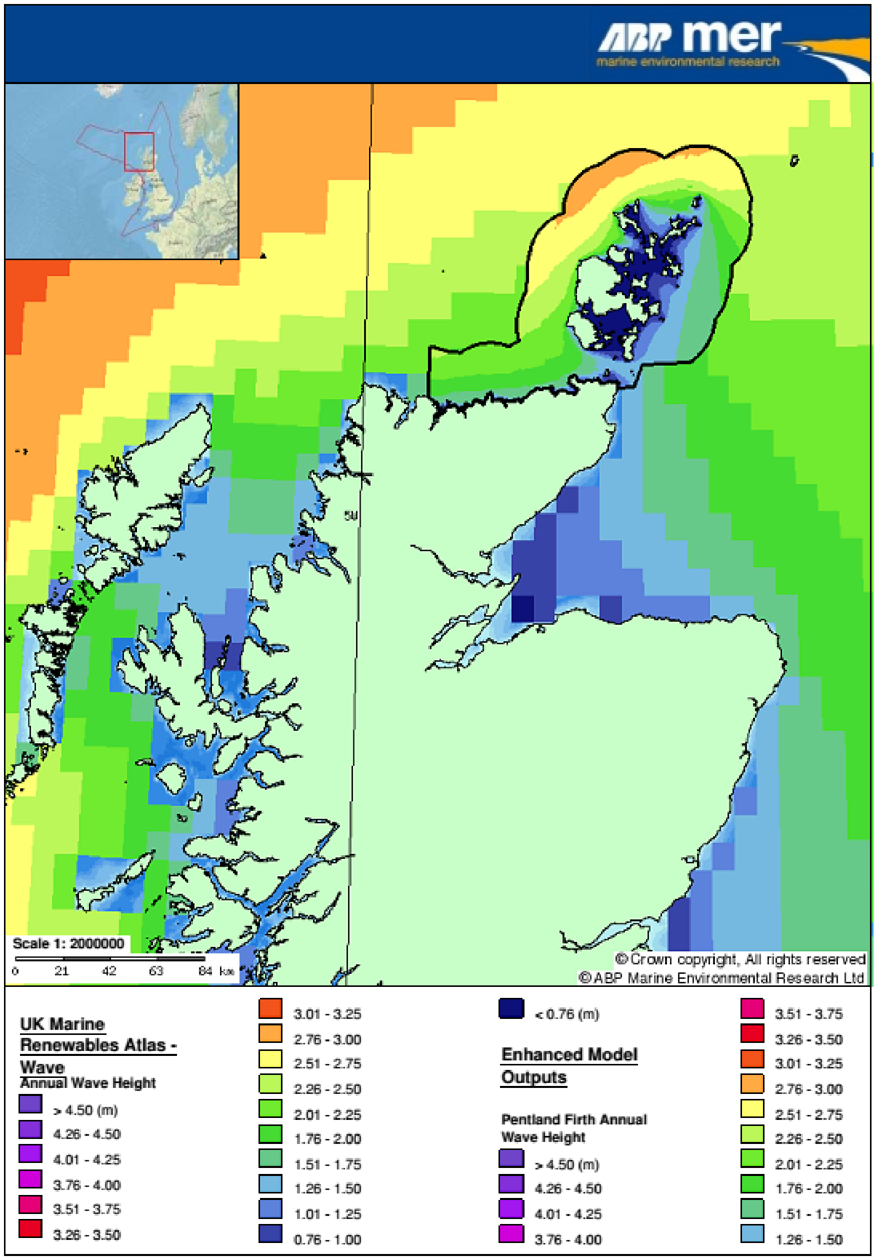

Figure 25. Annual significant wave height extracted from Atlas of UK Marine Renewable Energy Resources [ABPmer, 2008], *Reproduced from http://www.renewables-atlas.info/ © Crown Copyright.*

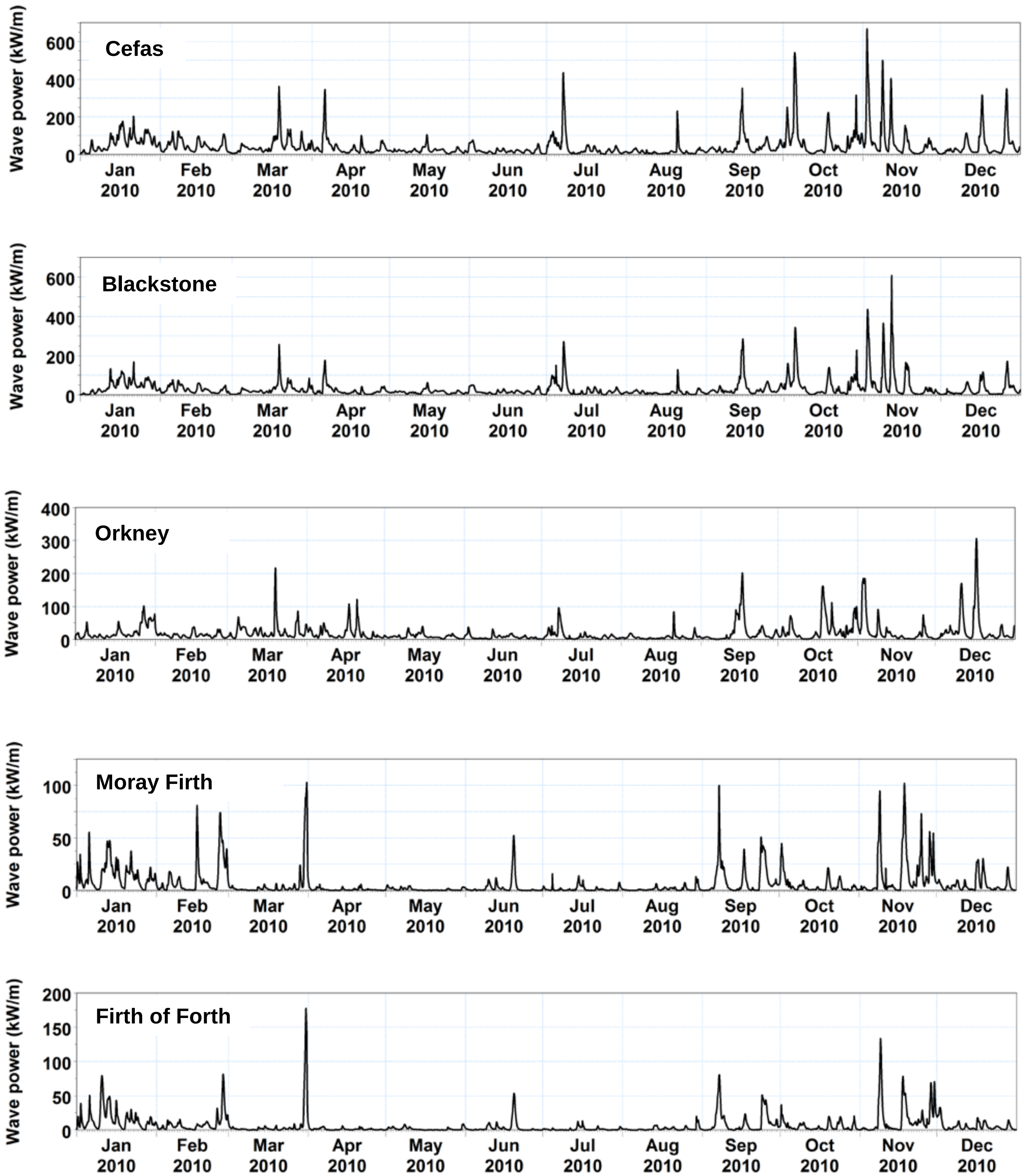

Figure 26(a). Wave power computed January-December 2010, from top to bottom, for Cefas, Blackstone, Orkney, Moray Firth and Firth of Forth.

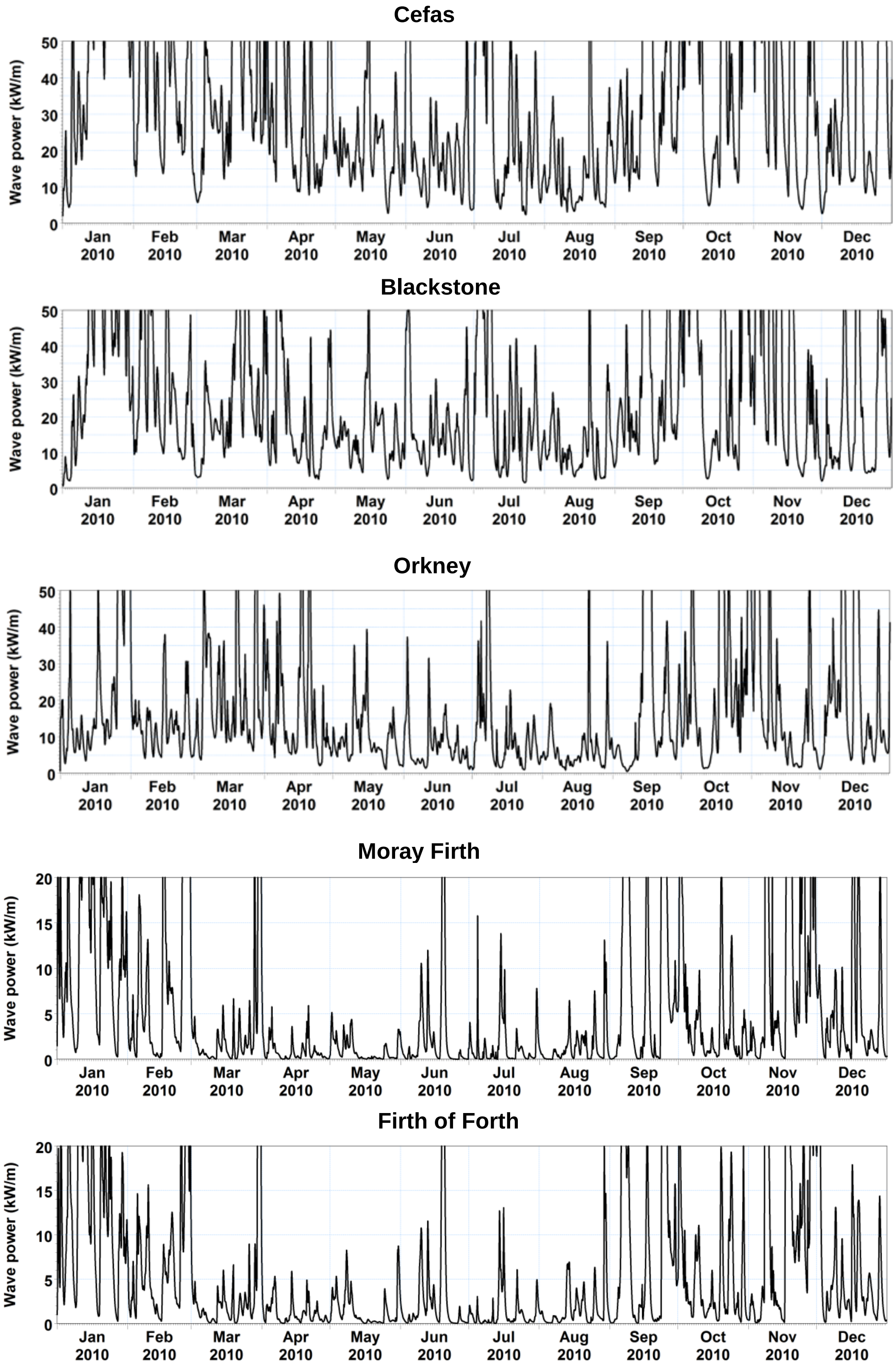

Figure 26(b). Wave power computed January-December 2010. Same as in Figure 26 (a), but with enlarged vertical scale: Cefas, Blackstone, Orkney, Moray Firth and Firth of Forth.

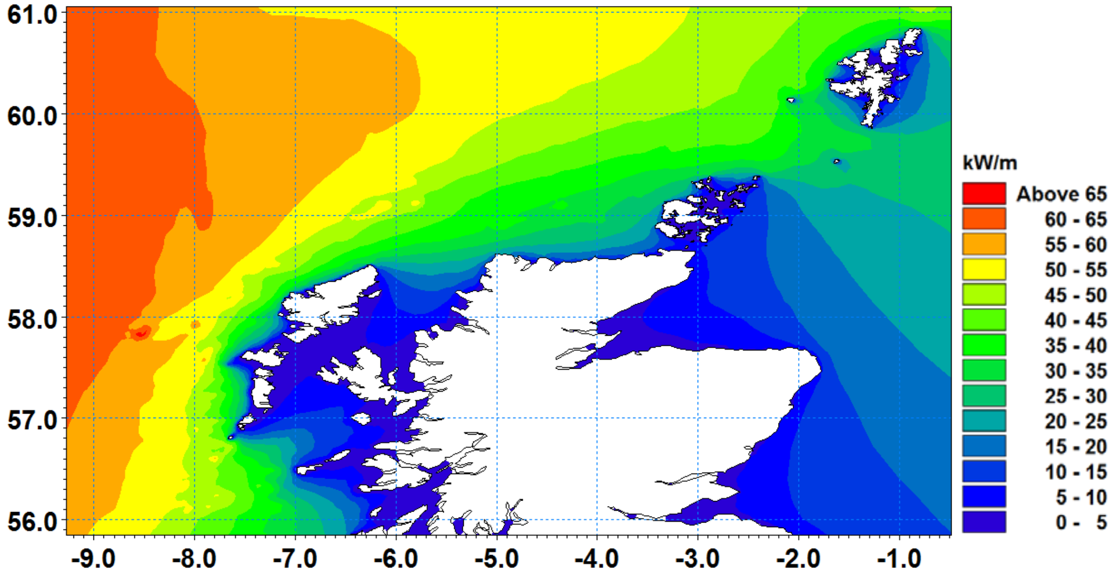

Figure 27. Mean wave power for January-December 2010

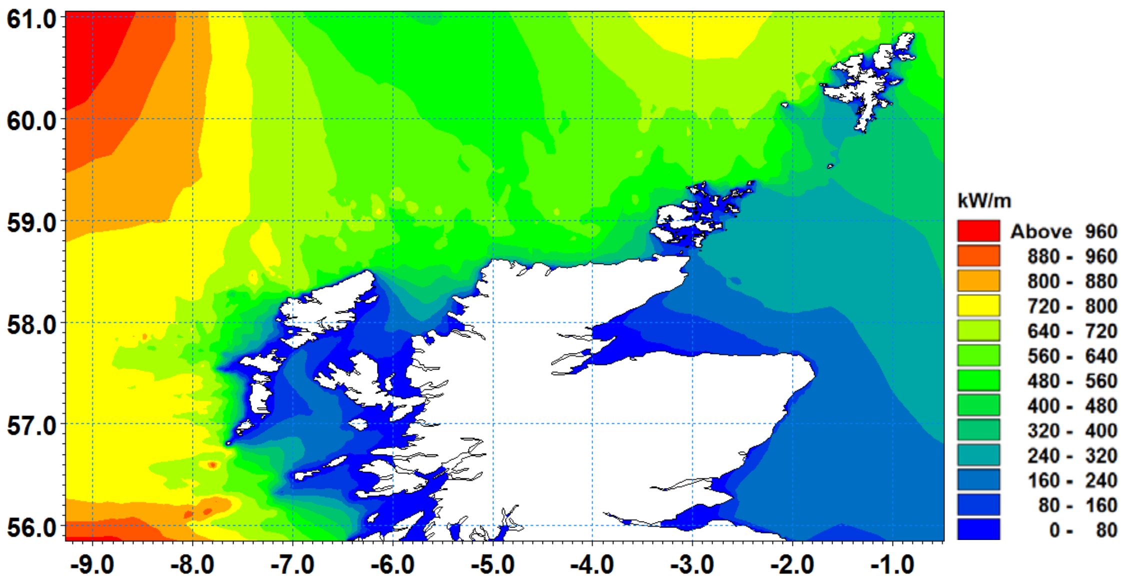

Figure 28. Maximum wave power for January-December 2010

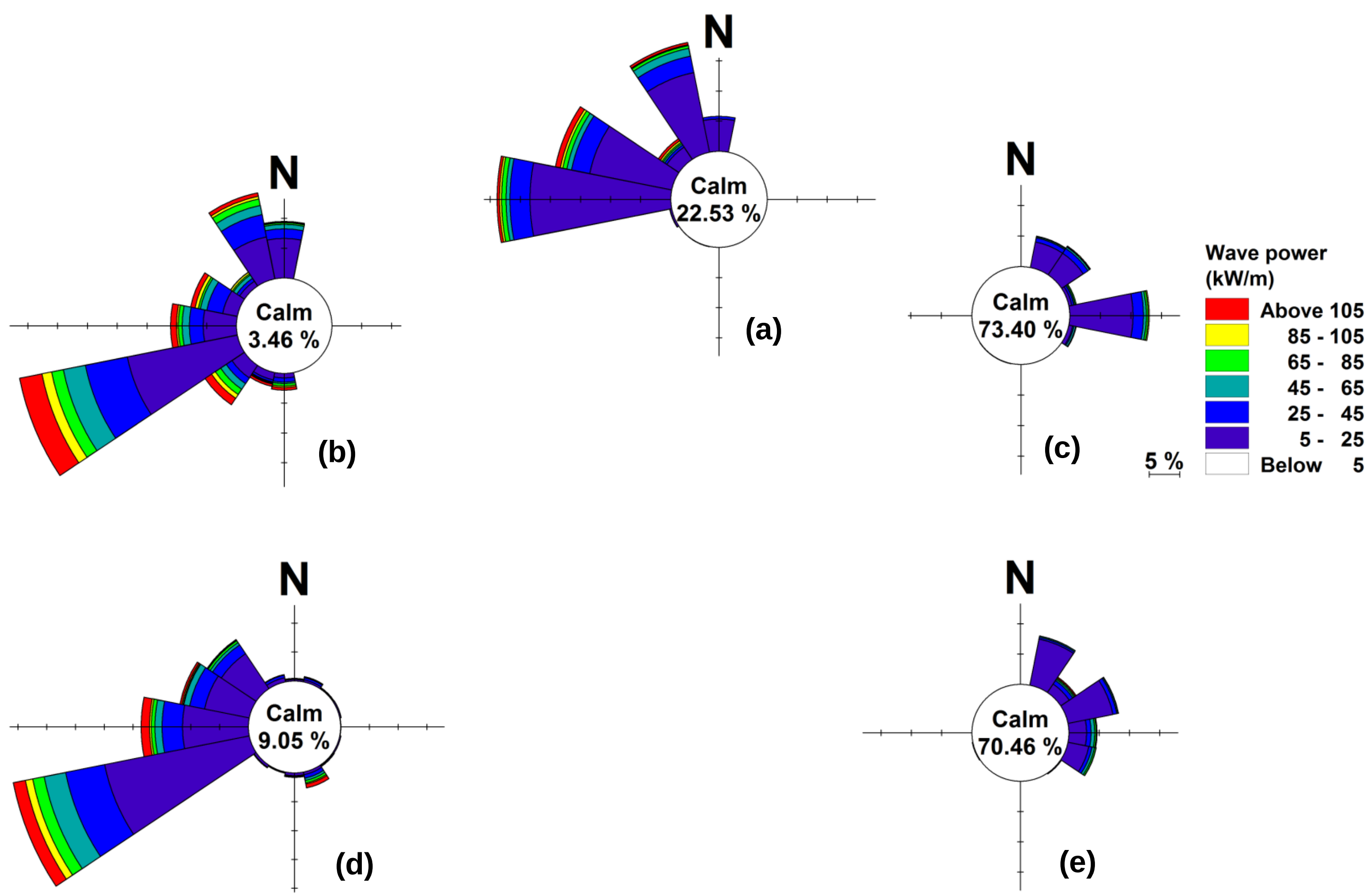

Figure 29. Rose plots for wave power with peak wave direction for different locations: (a) Orkney, (b) Cefas, (c) Moray Firth, (d) Blackstone and (e) Firth of Forth. Calculated from model results for January-December 2010.